Evaluation of Atomic Electron Binding Energies for Monte Carlo Particle Transport

Maria Grazia Pia, Hee Seo, Matej Batic, Marcia Begalli, Chan Hyeong Kim, Lina Quintieri, and Paolo Saracco

***Abstract*—A survey of atomic binding energies used by general purpose Monte Carlo systems is reported. Various compilations of these parameters have been evaluated; their accuracy is estimated with respect to experimental data. Their effects on physical quantities relevant to Monte Carlo particle transport are highlighted: X-ray fluorescence emission, electron and proton ionization cross sections, and Doppler broadening in Compton scattering. The effects due to different binding energies are quantified with respect to experimental data. Among the examined compilations, EADL is found in general a less suitable option to optimize simulation accuracy; other compilations exhibit distinctive capabilities in specific applications, although in general their effects on simulation accuracy are rather similar. The results of the analysis provide quantitative ground for the selection of binding energies to optimize the accuracy of Monte Carlo simulation in experimental use cases. Recommendations on software design dealing with these parameters and on the improvement of data libraries for Monte Carlo simulation are discussed.**

***Index Terms*—Geant4, ionization, Monte Carlo, PIXE, simulation, X-ray fluorescence.**

I. Introduction

THE simulation of particle interactions in matter involves a number of atomic physics parameters, whose values affect physics models applied to particle transport and experimental observables calculated by the simulation. Despite the fundamental character of these parameters, a consensus has not always been achieved about their values, and different Monte Carlo codes use different sets of parameters.

Atomic parameters are especially relevant to simulation scenarios that are sensitive to detailed modeling of the properties of the interacting medium. Examples include the generation of characteristic lines resulting from X-ray fluorescence or Auger electron emission, and precision simulation studies, such as microdosimetry, that involve the description of particle interactions with matter down to energies comparable with the scale of atomic binding energies.

Simulation in these domains has been for an extended time the object of specialized Monte Carlo codes; some general purpose Monte Carlo systems have devoted attention to these areas, introducing functionality for the simulation of fluorescence, PIXE (Particle Induced X-ray Emission) and microdosimetry. In this context, emphasis has been placed on the development and validation of the physics models implemented in the simulation systems, while relatively limited effort has been invested into verifying the adequacy of the atomic parameters used by general purpose Monte Carlo codes with regard to the requirements of new application domains.

This paper surveys atomic binding energies used by well known Monte Carlo systems, including EGS [1], EGSnrc [2], Geant4 [3], [4], ITS (Integrated Tiger Series) [5], MCNP/MCNPX [6], [7] and Penelope [8], and by some specialized physics codes. These software systems use a variety of compilations of binding energies, which are derived from experimental data or theoretical calculations; this paper investigates their accuracy and their effects on simulations.

II. Compilations of Electron Binding Energies

The binding energies considered in this study concern neutral atoms in their ground state; several compilations of their values, of experimental and theoretical origin, are available in the literature.

Compilations based on experimental data are the result of the application of selection, evaluation, manipulations (like interpolation and extrapolation) and semi-empirical criteria to available experimental measurements to produce a set of reference values covering the whole periodic system of the elements and the complete atomic structure of each element.

Most of the collections of electron binding energies based on experimental data derive from a review published by Bearden and Burr in 1967 [9]. Later compilations introduced further refinements in the evaluation of experimental data and the calculation of binding energies for which no measurements were available; they also accounted for new data taken after the publication of Bearden and Burr's review.

Experimental atomic binding energies can be affected by various sources of systematic effects; they originate not only from the use of different experimental techniques in the measurements, but also from physical effects: for instance, binding energies of elements in the solid state are different from those of

Manuscript received May 18, 2011; revised August 31, 2011; accepted October 10, 2011. Date of current version December 14, 2011.

M. G. Pia and P. Saracco are with the INFN Sezione di Genova, I-16146 Genova, Italy (e-mail: mariagrazia.pia@ge.infn.it; saracco@ge.infn.it).

H. Seo and C. H. Kim are with the Department of Nuclear Engineering, Hanyang University, Seoul 133-791, Korea (e-mail: shee@hanyang.ac.kr; chkim@hanyang.ac.kr).

M. Batic is with INFN Sezione di Genova, Genova, Italy, on leave from the Jozef Stefan Institute, 1000 Ljubljana, Slovenia (e-mail: matej.batic@ge.infn.it).

M. Begalli is with the State University of Rio de Janeiro, 20551-030 Rio de Janeiro, Brazil (e-mail: marcia.begalli@cern.ch.).

L. Quintieri is with the INFN Laboratori Nazionali di Frascati, I-00044 Frascati, Italy (e-mail: lina.quintieri@lnf.infn.it).

Color versions of one or more of the figures in this paper are available online at http://ieeexplore.ieee.org.

Digital Object Identifier 10.1109/TNS.2011.2172458

free atoms, and binding energy measurements can be affected by the chemical state of a solid.

The first attempt to calculate electron binding energies was reported by Slater [10]; since then, various relativistic computations of neutral atom binding energies have been performed [11]. They exploit methods based on a Dirac-Hartree-Slater model, with corrections for QED (quantum electrodynamics) effects and the nuclear charge distribution.

A. Selected Compilations

This paper evaluates a selection of binding energy compilations, which are used by general purpose simulation systems and some representative specialized codes:

- the compilation by Bearden and Burr [9],
- the compilation by Carlson [12],
- the tabulation included in Evaluated Atomic Data Library (EADL) [13],
- the compilation assembled by Sevier in 1979 [14],
- the compilations included in the seventh and eighth editions of the Table of Isotopes [15], [16], respectively published in 1978 and 1996,
- the compilation by Williams included in the X-ray Data Booklet [17] and in the CRC Handbook of Chemistry and Physics [18].

Bearden and Burr performed a comprehensive evaluation of experimental X-ray wavelength data; the techniques they used to establish a consistent energy scale and to deal with elements with multiple or missing measurements are documented in [9]. This compilation has been the basis for several other ones published in the following years and is still used in some physics software systems.

Carlson's compilation reproduces the one by Lotz [19] with a few modifications and extensions, that concern the data for krypton and xenon, the binding energies of elements with atomic number greater than 94 and the P shell data of elements with atomic number between 87 and 95. The compilation covers atomic numbers from 1 to 106; values are given for free atoms and are referenced to the vacuum potential.

The compilation by Lotz is based on Bearden and Burr's evaluated data, complemented by other experimental measurements. The tabulated binding energies were determined according to empirical criteria, interpolation and extrapolation of available data. Since values are listed for free atoms, the work function was taken into account in converting experimental binding energies for solids. According to [19], the uncertainties of the tabulated values are at most 2 eV for elements with atomic number up to 92; larger uncertainties, in some cases greater than 10 eV, are reported for heavier elements.

The binding energies collected in the seventh edition of the Table of Isotopes (identified in the following as ToI 1978) were taken from Shirley *et al.* [20] for elements with atomic number up to 30, and from a compilation of experimental data by the Uppsala Group [21] for heavier elements. The tabulated binding energies derive mainly from photoelectron spectroscopic measurements; data were taken from Bearden and Burr's compilation in cases where experimental photoelectron measurements were not available. Interpolation and extrapolation techniques were used to complement experimental data. The data are listed with reference to the Fermi level and concern elements with atomic number from 1 to 104. Uncertainties are reported as about 0.1 eV for light elements and 1–2 eV for most elements with atomic number greater than 30; uncertainties approaching 100 eV are mentioned for transuranic elements. Shifts of the order of 10 eV in the binding energy of non-valence shells can result from changes in the chemical state of the medium [20].

The binding energies collected in the eighth edition of the Table of Isotopes (identified in the following as ToI 1996) were taken from the compilation by Larkins [22]. Binding energies are reported for solid systems referenced to the Fermi level, except those for noble gases, Cl and Br, which are for vapor phase systems referenced to the vacuum level. Uncertainties may be as large as 10–20 eV for the inner orbitals in the high-Z elements, and changes in chemical state can lead to substantial shifts in the binding energies of non-valence shells [20].

The binding energies tabulated by Larkins are based on Sevier's 1972 compilation [23] for elements with atomic number up to 83 and on the compilation by Porter and Freedman [24] for heavier elements; with respect to these references, Larkins includes some updated values for Ar, Ge, As, Se, Xe and Hg. Sevier's 1972 tabulations were mainly an update to Bearden and Burr's ones to include more recent measurements; a further extension was published by Sevier in 1979 [14]. Porter and Freedman combined a theoretical approach and experimental measurements to interpolate data for heavy elements.

The eighth edition of the Table of Isotopes also includes a list of ionization energies of the elements (concerning the least bound electron), which reflects the data available from NIST (United States National Institute of Standards and Technology) [25]; these values differ in some cases from those in the tabulation of electron binding energies in the same volume.

Williams' compilation is based on Bearden and Burr's data; some values are taken from [30] with additional corrections, and some from [31]. The energies are given relative to the vacuum level for the rare gases and for H, N, O, F and Cl, relative to the Fermi level for metals and relative to the top of the valence bands for semiconductors. The tabulations concern elements with atomic number between 1 and 92.

The atomic subshell parameters collected in EADL are derived from theoretical calculations by Scofield [26], [27]; besides these two references, EADL documentation cites a "private communication" by Scofield, dated 1988, as a source of the data. Due to the scarcity of documentation about the origin of the binding energies listed in EADL, it is difficult to ascertain how they were calculated, and what assumptions and approximations may be underlying. Binding energy values, although not for all elements and shells of the periodic system, are reported in some publications by Scofield [28], [29]; those in [29] appear consistent with EADL tabulations. EADL data concern isolated, neutral atoms with atomic number up to 100.

B. Binding Energies Used by Physics Software Systems

General purpose Monte Carlo systems and specialized codes use a variety of binding energy compilations.

EGS5 uses the binding energies tabulated in the 1996 edition of the Table of Isotopes, while EGSnrc uses the values of the earlier 1978 edition, as EGS4 [32] did.

MCNP, MCNPX and ITS use the electron binding energies compiled by Carlson.

The Penelope 2008 version uses Carlson's compilation of binding energies; earlier versions used the compilation included in the 1978 edition of the Table of Isotopes.

The Geant4 toolkit uses various collections of binding energies. The main reference for binding energies in Geant4 is the *G4AtomicShells* class in the *materials* package;

according to comments in the code implementation, the binding energies values in it derive from Carlson's compilation and the 73rd edition of the CRC Handbook of Chemistry and Physics [33].

EADL values are used by the implementations of photon and electron interactions in Geant4 low energy electromagnetic package [34], [35] based on the so-called Livermore Library, which encompasses the Evaluated Electron Data Library (EEDL) [36], the Evaluated Photon Data Library (EPDL97) [37] and EADL itself. EADL binding energies are also used in the calculation of proton ionization cross sections described in [38] and released in Geant4 9.4 in a modified version [39] to address the drawbacks documented in [40]. Proton ionization cross sections for Geant4 PIXE (Particle Induced X-ray Emission) simulation described in [40] derive from ISICS [41] tabulations using Bearden and Burr's binding energies.

Geant4 includes a C++ reimplementation of physics models originally implemented in Penelope; Geant4 9.4 reimplements models from the 2008 version of Penelope, while previous Geant4 releases included models equivalent to Penelope 2001. The Geant4 9.4 reimplementation appears to use EADL values instead of the binding energies used by Penelope 2008. Binding energies corresponding to the values in the 1978 edition of the Table of Isotopes are included in a Geant4 9.4 data set associated with Penelope.

Ionization energies consistent with those reported by NIST [25] are included in Geant4 *G4StaticSandiaData* class.

No reference to atomic binding energies can be retrieved in GEANT 3 documentation; however, according to comments embedded in the code, GEANT 3 used Bearden and Burr's binding energies, with updated values for xenon derived from [43]. Nevertheless, the *GSHLIN* subroutine, where binding energies are hard-coded, exhibits some discrepancies with respect to both Bearden and Burr's tabulations and the values in [43]; the origin of these values could not be retrieved in the literature, nor in the software documentation. Presumably, the code implementation and its comments went out of phase at some stage of GEANT 3 evolution.

Atomic binding energies are relevant to PIXE calculations; two well known software systems pertinent to this domain are GUPIX [44] and ISICS [41]. GUPIX uses Sevier's 1979 compilation of binding energies [45], which includes extensions to the 1972 collection by the same author. ISICS uses Bearden and Burr's binding energies by default; the most recent version of the code [46] offers the option of using the binding energies assembled in Williams's compilation instead of Bearden and Burr's ones.

The authors of this paper could not retrieve track of the electron binding energies used by FLUKA in the related software documentation and in the literature, nor from direct inquiries with the maintainers of the code; it was not possible to ascertain them from the software implementation, whose disclosure is subject to restrictions, as their presumed source file is in a binary encoded format.

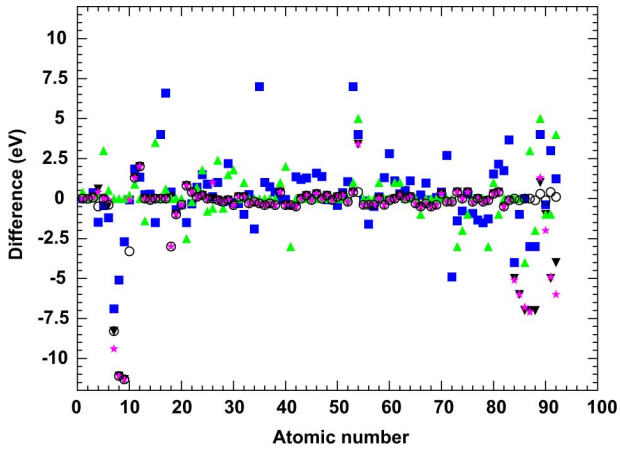

Fig. 1. Difference between K shell binding energies in various compilations and binding energies in Williams' one versus atomic number: Carlson (blue squares), Table of Isotopes 1996 (black down triangles), Table of Isotopes 1978 (green up triangles), Sevier 1979 (pink stars), Bearden and Burr (empty circles). EADL binding energies are shown in Fig. 2, due to the large difference of scale with respect to the values plotted in this figure.

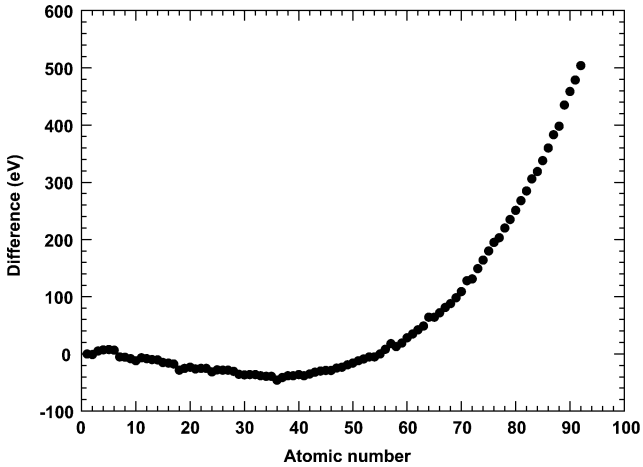

Fig. 2. Difference between K shell binding energies in EADL and in Williams' compilation versus atomic number.

C. Comparison of Binding Energies Compilations

The binding energies collected in the various compilations exhibit some differences, apart from those due to different references—the vacuum potential or the Fermi level.

A few examples of comparison are displayed in Figs. 1–7; the plots show the difference between the binding energies in the various compilations and the values in Williams' compilation. The choice of Williams' compilation as a reference for plotting differences is arbitrary; the main qualitative features of the plots are equivalent, if other empirical compilations are chosen as a reference instead of Williams' one. The difference between

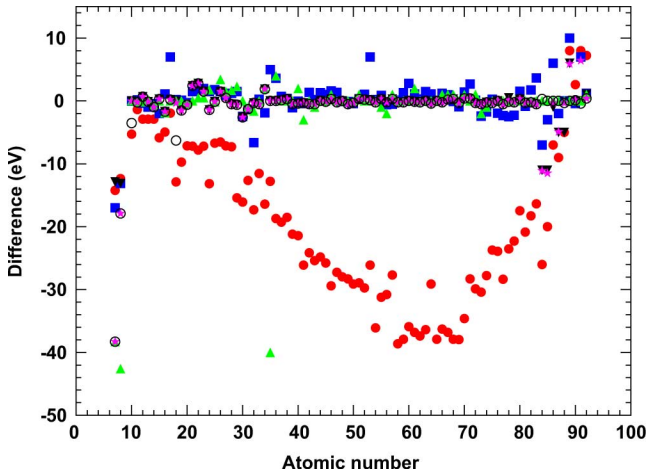

Fig. 3. Difference between L_1 shell binding energies in various compilations and binding energies in Williams' one versus atomic number: EADL (red circles), Carlson (blue squares), Table of Isotopes 1996 (black down triangles), Table of Isotopes 1978 (green up triangles), Sevier 1979 (pink stars), Bearden and Burr (empty circles).

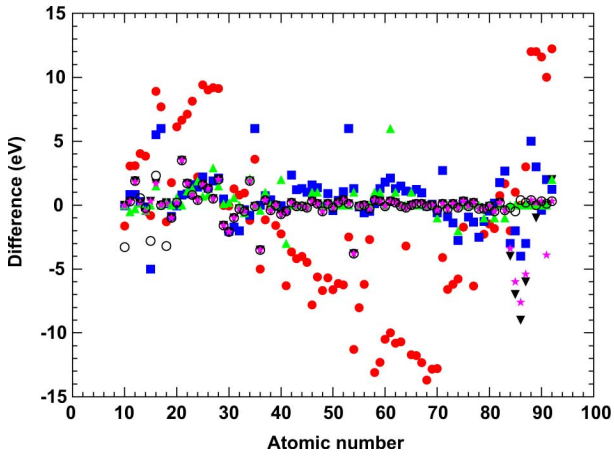

Fig. 5. Difference between L_3 shell binding energies in various compilations and binding energies in Williams' compilation versus atomic number: EADL (red circles), Carlson (blue squares), Table of Isotopes 1996 (black down triangles), Table of Isotopes 1978 (green up triangles), Sevier 1979 (pink stars), Bearden and Burr (empty circles).

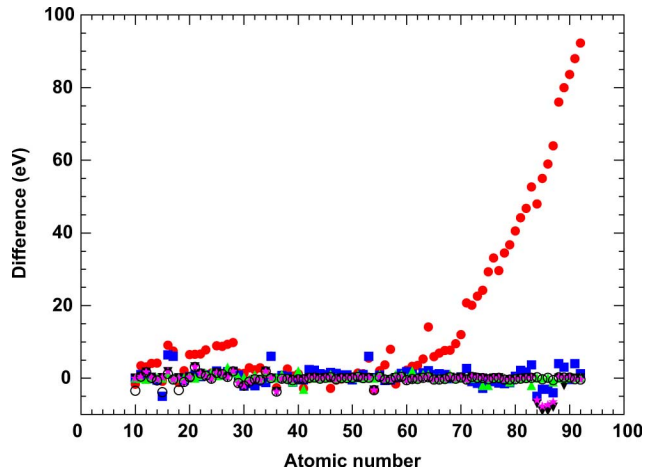

Fig. 4. Difference between L_2 shell binding energies in various compilations and binding energies in Williams' compilation versus atomic number: EADL (red circles), Carlson (blue squares), Table of Isotopes 1996 (black down triangles), Table of Isotopes 1978 (green up triangles), Sevier 1979 (pink stars), Bearden and Burr (empty circles).

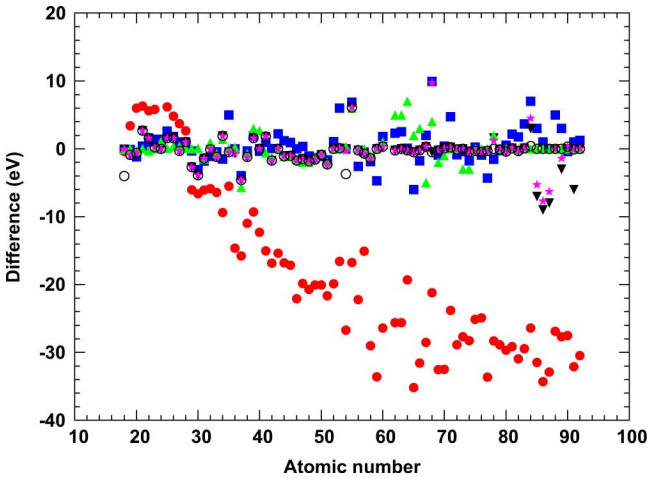

Fig. 6. Difference between M_1 shell binding energies in various compilations and binding energies in Williams' compilation versus atomic number: EADL (red circles), Carlson (blue squares), Table of Isotopes 1996 (black down triangles), Table of Isotopes 1978 (green up triangles), Sevier 1979 (pink stars), Bearden and Burr (empty circles).

EADL and Williams' K shell binding energies is plotted separately from the other compilations, since the scale is approximately a factor 30 larger.

The differences are of the order of a few electronvolts across the various empirical compilations, as illustrated in Fig. 1, while they are larger between EADL and the empirical compilations, especially for inner shells, as shown in Fig. 2; they can reach a few hundred electronvolts for the K shell of heavier elements. The empirical compilations derive from a common source (Bearden and Burr's review); therefore it is not surprising that they exhibit some similarities.

III. Strategy of the Study

The study documented in this paper is driven by pragmatic motivations. The analysis is focused on quantifying the accuracy of binding energy compilations used in Monte Carlo systems, and their impact on physics models of particle transport and on experimental observables produced by the simulation. The evaluation aims at identifying one or more optimal options for Monte Carlo applications in experimental practice. A comprehensive review of the physical ground, experimental measurements and methods of calculations of electron binding energies is outside the scope of this paper.

Two complementary approaches are adopted: direct validation of tabulated electron binding energy values and the evaluation of effects on related physics quantities, like ionization cross sections and X-ray fluorescence emission. Both analyses involve comparisons with experimental data and a comparative appraisal of the accuracy of the various compilations. The set of related physics quantities examined in the paper reflects the use of electron binding energies in Geant4, which concerns the calculation of the energy of fluorescence X-rays and Auger electrons, the simulation of Compton scattering with bound electrons and the computation of proton ionization cross sections,

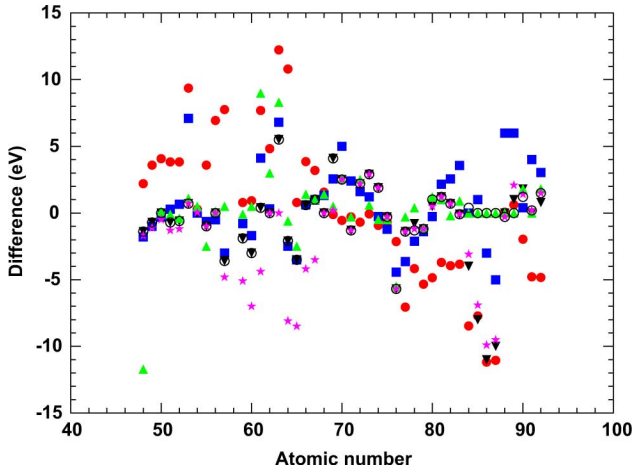

Fig. 7. Difference between N_5 shell binding energies in various compilations and binding energies in Williams' compilation versus atomic number: EADL (red circles), Carlson (blue squares), Table of Isotopes 1996 (black down triangles), Table of Isotopes 1978 (green up triangles), Sevier 1979 (pink stars), Bearden and Burr (empty circles).

with the exception of the use of electron binding energies in the simulation of the photoelectric effect, whose validation is intended to be covered in a dedicated paper. The use in Geant4 can be considered representative of the role of atomic binding energies in general purpose Monte Carlo codes. In addition, the paper examines the effect of atomic binding energies in the calculation of recently developed electron ionization cross sections, which are intended for inclusion in Geant4, but have not been publicly released yet.

The study is articulated over a variety of test cases, which involve different physics issues and reference data; the analysis methods are tailored to the physical and experimental features of each test case. Various statistical tools are exploited to quantify the accuracy of the distributions examined in this study and the difference (or equivalence) of the various binding energy compilations.

Goodness-of-fit tests mentioned in the following sections utilize the Statistical Toolkit[49], [50]. Whenever applicable, multiple goodness-of-fit tests are applied to mitigate the risk of systematic effects in the conclusions of the analysis due to peculiarities of the mathematical formulation of the various methods.

A combination of Student's t-test and F-test is applied to study the distribution of differences between the data subject to evaluation and reference values, when goodness-of-fit tests do not exhibit adequate discriminant power over some analyzed data samples. The t-test is utilized to estimate the compatibility with null mean difference, while, once the sample exhibiting the narrowest distribution of differences (i.e., the lowest variance) has been singled out, the F-test is used to identify the data samples whose variance is statistically equivalent to the narrowest distribution.

The binding energies listed in the various compilations are given with respect to different references (vacuum or Fermi level). In the following comparisons the original values are corrected to account for the work function as appropriate to ensure a consistent reference. Values of the work function are taken from the compilation of the CRC Handbook of Physics and Chemistry [18], which is considered an authoritative source for these data in experimental practice; they are complemented by data from [51] and [52] for elements not included in the compilation of [18].

The analyses reported in the following sections concern elements with atomic number between 1 and 92, unless differently specified. This range ensures uniform treatment of the various compilations in their comparative appraisal, since all the examined compilations cover these elements, while only a subset of them deal with transuranic elements. Moreover, established experimental references of transuranic elements suitable for the analysis of binding energies are scarce.

IV. Evaluation of Reference Binding Energies

Comparison with experimental data is the prime method to evaluate the accuracy of simulation models; this validation method requires reliable experimental measurements as a reference. Three authoritative collections of experimental binding energies (two of which are partially overlapping) are used for this purpose; they include values for a limited number of elements and shells, therefore they can validate only part of the content of the compilations mentioned in the previous sections.

A. Comparison With High Precision Reference Data

Experimental values of elemental binding energies reported in the literature exhibit significant discrepancies [53]; they can affect the validation of binding energy compilations.

Inconsistencies in the measurements are mostly due to inadequacies in the calibration of binding energy scales of the various instruments, and are often visible when comparing measurements performed by different laboratories.

Binding energy measurements may differ also for physical reasons: elemental binding energies differ in the vapour and condensed states, and a chemical shift is present when atoms are investigated in chemical compound states. Moreover, binding energies for atoms implanted by ion bombardment into a metal foil substrate are shifted with respect to those for a foil of the pure element. Measurements on different surfaces of a crystal can result in different ionization energy values.

These effects may be sources of systematic errors, which can be significant when comparing the binding energies collected in the various compilations with experimental values.

A further source of uncertainties derives from the conversion between binding energy values of solids referenced to the Fermi level and to the vacuum level; this operation involves adding, or subtracting, the value of the work function.

A collection of high precision binding energies [54] was assembled by Powell for the purpose of constituting a reference for the NIST X-ray Photoelectron Spectroscopy Database [55]. Data published by different laboratories were subject to a retroactive calibration procedure; the original experimental values were corrected to produce a set of 61 binding energy values, concerning elements with atomic numbers between 4 and 84 and shells from K to N. The uncertainty of the reference energies is reported to be 0.061 eV [54]. These high precision data have been used to evaluate the accuracy of the binding energy compilations examined in this study.

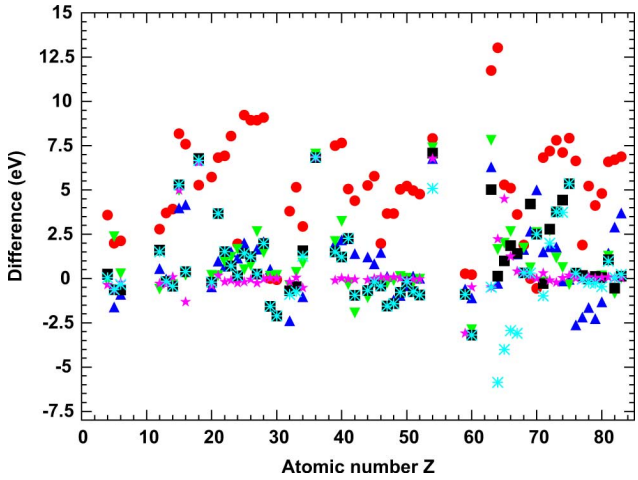

Fig. 8. Difference between binding energies in various compilations and reference data from [54] versus atomic number: EADL (red circles), Carlson (blue up triangles), Table of Isotopes 1996 (black squares), Table of Isotopes 1978 (green down triangles), Williams (pink stars), Sevier 1979 (turquoise asterisks).

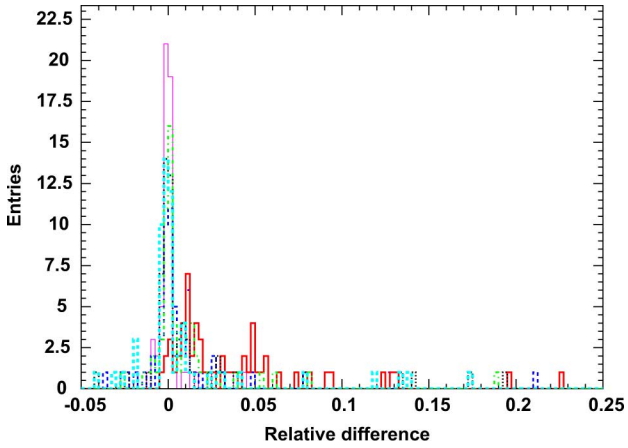

Fig. 9. Relative difference between binding energies in various compilations and reference data from [54]: Carlson (dashed blue line), Table of Isotopes 1996 (dotted black line), Table of Isotopes 1978 (dotted-dashed green line), Williams (thin pink solid line), Sevier 1979 (thick turquoise dashed line) and EADL (thick solid red line).

The difference of the binding energies in the various compilations with respect to the reference values of [54] is shown in Fig. 8; the relative difference with respect to the same data is shown in Fig. 9. EADL binding energies appear less accurate than the samples from other compilations and exhibit a systematic shift with respect to the reference values.

Goodness of fit tests, which are commonly applied in statistical analysis to compare data distributions, do not appear adequate to discriminate the compatibility of the various compilations with respect to the reference data of [54].

Goodness of fit tests based on the empirical distribution function (Kolmogorov-Smirnov[56], [57], Anderson-Darling [58], [59] and Cramer-von Mises [60], [61]) result in p-values greater than 0.999 for all the data samples: this means that the differences between the binding energies of the various compilations and the reference data are small with respect to the sensitivity of these tests to detect discrepancies in the distributions subject to comparison. It is worthwhile to remark that the power of goodness-of-fit tests is still a subject of research in statistics.

On the other hand, the χ^2 statistic [62] based on the uncertainties of the reference data reported in [54] (0.061 eV) results in p-values much smaller than 0.001 for all the binding energy samples; therefore the χ^2 test would reject the hypothesis of compatibility of any compilation with the reference data sample with 0.001 significance.

The outcome of the χ^2 test depends critically on the correct estimate of the uncertainties of the data subject to test. The procedure applied in [54] to build the reference data sample mitigates the risk of possible systematic effects due to instrumental calibration, which may affect raw experimental data; nevertheless, other sources, independent from the intrinsic precision of the measurement, may contribute to the overall uncertainty.

Previously mentioned physical and chemical shifts of the experimental data, associated with the conditions of the measurements, may introduce systematic effects. In this context, one should take into account that, while the reference values in [54] reflect the experimental configuration and instrumental energy resolution for each measured material, the data tabulated in the various empirical compilations are the result of manipulations, such as interpolations, extrapolations and fits, over large collections of heterogeneous experimental data from multiple sources: the generic binding energy estimates deriving from these procedures may not adequately account for the peculiarities of experimental measurements performed in specific physical and chemical configurations. The calculation of the χ^2 test statistic includes only the uncertainties associated with Powell's reference data; it does not account for errors associated with the binding energies of the various compilations.

A further source of uncertainty is associated with the work function in cases where a conversion between the Fermi and vacuum reference level should be applied for consistency between the distributions subject to comparison. Moreover, experimental values of the work function are affected by the technique of measurement and the cleanliness of the surface. The CRC compilation does not report the uncertainties of the work functions; therefore this additional error cannot be included in the computation of the χ^2 test statistic concerning Carlson's and EADL binding energies.

Due to these considerations, caution should be exercised in interpreting the outcome of the χ^2 test as physically significant, as the nominal uncertainties values involved in the calculation may not realistically represent the actual uncertainties associated with the tested data samples.

Other statistical methods than goodness-of-fit testing were exploited to quantify the compatibility between the various binding energies compilations and the reference data of [54].

A Student's t-test was performed to estimate whether the differences between the binding energies of the various compilations and the corresponding reference values are compatible with a true mean of zero. The p-values resulting from this test are summarized in Table I. The binding energies of Williams' and 1979 Sevier's compilations are compatible at 0.05 level of significance with null mean difference with respect to the reference data; the t-test rejects the hypothesis of compatibility with zero

TABLE I
STUDENT'S T-TEST APPLIED TO THE DIFFERENCE WITH RESPECT TO POWELL'S REFERENCE DATA

Compilation	All data		Excluding Ar, Xe, Kr	
	Mean (eV)	p-value	Mean (eV)	p-value
Bearden and Burr	0.51	0.026	0.40	0.083
Carlson	0.95	0.001	0.65	0.008
EADL	4.85	<0.0001	4.75	<0.0001
Sevier 1979	0.41	0.181	0.11	0.673
ToI 1978	1.00	0.0004	0.69	0.002
ToI 1996	0.99	0.001	0.69	0.006
Williams	0.41	0.076	0.09	0.545

TABLE II
F-TEST APPLIED TO THE DIFFERENCES WITH RESPECT TO POWELL'S REFERENCE DATA

Compilation	Standard deviation (eV)	p-value
Bearden and Burr	1.71	0.0005
Carlson	1.80	0.0001
EADL	1.56	0.005
Sevier 1979	2.01	<0.0001
ToI 1978	1.61	0.002
ToI 1996	1.84	0.0001
Williams	1.07	-

mean difference with 0.01 significance for all the other compilations. It should be stressed that these tests, as well as similar ones reported in the following, do not compare the compilations with each other, but how well they reproduce the set of precision reference data.

All the binding energies compilations exhibit rather large differences with respect to the reference data for rare gases (Ar, Xe and Kr) reported in [54], that derive from implants in other media. If one excludes these data from the t-test, also Bearden and Burr's binding energies are compatible with zero mean difference with respect to the reference data at 0.05 significance level.

The binding energies of Williams' compilation exhibit the narrowest distribution of differences with respect to the reference data of [54], as can be seen in Fig. 9. The standard deviations related to the various compilations are listed in Table II, excluding the data for argon, xenon and krypton, which are treated as outliers. The table also reports the p-values of the F-test to evaluate the hypothesis of equality of variance associated with the various compilations with respect to the binding energies of Williams' compilation; the distributions subject to the F-test concern the difference between the binding energies in the compilations and the reference data of [54]. The statistical analysis confirms the qualitative evidence of Fig. 9, since the null hypothesis is rejected with 0.01 significance level for all the test cases.

B. Comparison With NIST Recommended Binding Energies

A similar analysis has been performed with respect to the collection of recommended binding energies for principal photoelectron lines assembled by NIST [63]. This collection consists of 85 values; it includes most of the reference binding energies discussed in [54], along with additional data, mainly concerning outer shells other than those reported in [54]. The data for noble gases listed in [54] are not included in this set of recommended values.

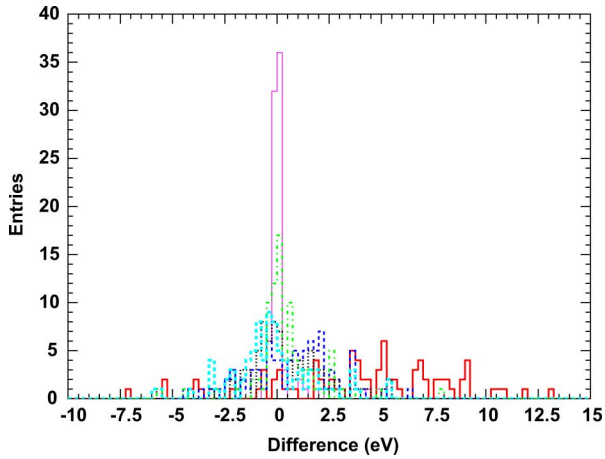

Fig. 10. Difference between binding energies in various compilations and reference data from [63]: Carlson (dashed blue line), Table of Isotopes 1996 (dotted black line), Table of Isotopes 1978 (dotted-dashed green line), Williams (thin pink solid line), Sevier 1979 (thick turquoise dashed line) and EADL (thick solid red line).

TABLE III
STUDENT'S T-TEST APPLIED TO THE DIFFERENCE WITH RESPECT TO NIST RECOMMENDED BINDING ENERGIES

Compilation	Mean (eV)	p-value
Bearden and Burr	0.35	0.070
Carlson	0.75	0.0003
EADL	3.96	<0.0001
Sevier 1979	-0.19	0.387
ToI 1978	0.44	0.017
ToI 1996	0.52	0.012
Williams	0.11	0.246

Fig. 10 shows the difference between the binding energies of the various compilations and the NIST recommended values.

The comparison with these reference data adopts a similar method to the one described in the previous section.

The p-values resulting from Student's t-test for compatibility with zero mean difference with respect to the reference data are reported in Table III. The binding energy samples extracted from the Williams' and Sevier's 1979 compilations are compatible with zero mean difference at 0.05 level of significance; those from the two editions of the Table of Isotopes are compatible at 0.01 level. Similarly to the previous case, the distribution of differences with the lowest standard deviation is the one associated with Williams' compilation.

The standard deviations of the distributions of differences from the reference data are reported for all the data samples in Table IV, together with the p-values of the F-test for the equality of variance with respect to the distribution associated with Williams' compilation. Consistently with the qualitative features of Fig. 10, the variance associated with Williams' binding energies is incompatible with the variance related to the other compilations.

Based on this statistical analysis, one can conclude that Williams' compilation best reproduces experimental reference binding energies. It should be stressed, however, that the NIST reference sample represents a small subset of the periodic system of elements: approximately 6% of the total number of shells of elements with atomic number up to 92.

TABLE IV
F-TEST APPLIED TO THE DIFFERENCE WITH RESPECT TO NIST RECOMMENDED BINDING ENERGIES

Compilation	Standard deviation (eV)	p-value
Bearden and Burr	1.74	<0.0001
Carlson	1.94	<0.0001
EADL	4.14	<0.0001
Sevier 1979	2.03	<0.0001
ToI 1978	1.66	<0.0001
ToI 1996	1.86	<0.0001
Williams	0.88	-

C. Evaluation of Ionization Energies

The ionization energy (in the past referred to as ionization potential), is the least energy that is necessary to remove an electron from a a free, unexcited, neutral atom, or an additional electron from an ionized atom. In the following analysis it is considered to be equal to the binding energy of the least bound electron in the atom.

A compilation of reference experimental ionization potentials is available from NIST [25]; the same values are also reported in the Table of Isotopes [15] in a table distinct from the compilation of electron binding energies and in the CRC Handbook of Chemistry and Physics [18]. This compilation does not list the uncertainties of the ionization energies it collects, but NIST web site comments that they range from less than one unit in the last digit of the given values to more than 0.2 eV.

The lowest binding energies for each element in the various compilations have been compared to the reference ionization energies collected by NIST. The compilations of the 1978 edition of the Table of Isotopes and Williams do not include many outer-shell binding energies; this limitation may be related to the emphasis of these compilations on experimental effects related to inner shells, like measurements concerning X-ray fluorescence or Auger electron emission. Therefore the following analysis was restricted to the compilations of Bearden and Burr, Carlson, EADL, Sevier 1979 and 1996 edition of the Table of Isotopes, which list a full set of electron binding energies.

The difference between ionization energies derived from the various compilations and NIST reference data is shown in Fig. 11. Carlson's binding energies appear to be in closest agreement with NIST ionization energies.

Goodness of fit tests are sensitive to the differences exhibited by the various compilations with respect to the NIST reference collection. The results of the Kolmogorov-Smirnov, Anderson-Darling and Cramer-von Mises tests are listed in Table V. The hypothesis of compatibility with NIST reference data is rejected by all the tests with 0.001 significance for EADL and Bearden and Burr's data. Carlson's compilations and the Table of Isotopes 1996 are compatible with the reference data at 0.05 significance level according to all the tests. Regarding Sevier's 1979 compilation, the Anderson-Darling test rejects the hypothesis of compatibility at 0.05 significance level, while the Kolmogorov-Smirnov and Cramer-von Mises test do not; the different response of these tests near the critical region of 0.05 significance could be explained by the greater sensitivity of the Anderson-Darling test statistic to fat tails.

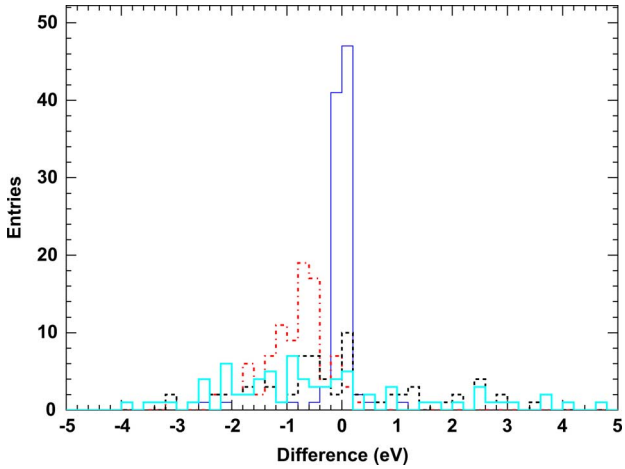

Fig. 11. Difference between ionization energies in various compilations and NIST reference experimental data: Carlson (thin solid blue line), Table of Isotopes 1996 (dashed black line), Sevier 1979 (thick solid turquoise line) and EADL (dot-dashed red line).

TABLE V
P-VALUES FROM GOODNESS-OF-FIT TESTS CONCERNING NIST REFERENCE IONIZATION POTENTIALS

Compilation	Kolmogorov Smirnov	Anderson Darling	Cramer von Mises
Bearden and Burr	<0.001	<0.001	<0.001
Carlson	0.670	0.995	0.963
EADL	<0.001	<0.001	<0.001
Sevier 1979	0.061	0.023	0.067
ToI 1996	0.096	0.099	0.213

V. EFFECTS ON FLUORESCENCE X-RAY ENERGIES

Compilations of characteristic X-ray energies are available, at least for lines of experimental interest, which in principle could be used in Monte Carlo simulation to determine the energy of secondary products of atomic relaxation. Nevertheless, these experimental tabulations can hardly satisfy the requirements of general purpose Monte Carlo codes, which require the ability of generating any atomic transition for any element. The energies of X-rays and Auger electrons resulting from atomic relaxation are often computed by Monte Carlo codes as the difference between the binding energies of the shells involved in the transition; in this approximation the binding energies of the atom in an ionised state are assumed to be the same as in the ground state. Therefore the accuracy of the simulation of the secondary products of atomic relaxation is determined by the accuracy of the binding energies implemented in the Monte Carlo system (apart from the physical approximation of neglecting the difference between the binding energies of an ionised atom and a neutral one in the ground state).

The accuracy of the examined binding energy compilations to reproduce the energy of atomic relaxation products has been estimated with respect to the experimental X-ray energies reported in the review by Deslattes *et al.* [64], which concerns K and L transitions.

A comparison of X-ray energies calculated by Geant4, based on EADL binding energies, with respect to the same experimental data is documented in [65]. That study showed that, according to the outcome of the Kolmogorov-Smirnov test, all the

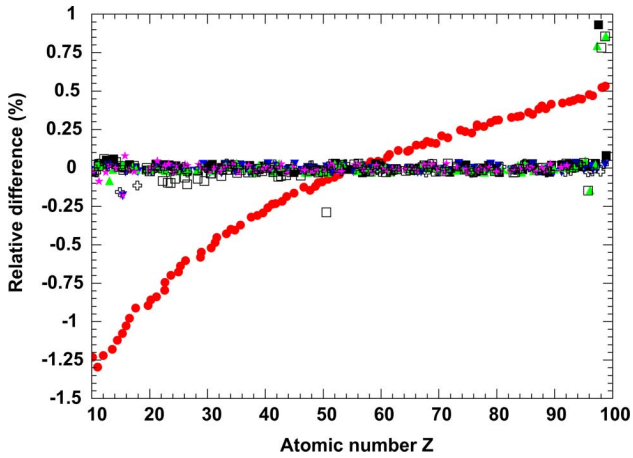

Fig. 12. KL_2 transition, relative difference between binding energies in various compilations and experimental data from [64] versus atomic number: EADL (red circles), Carlson (blue up triangles), Table of Isotopes 1996 (black squares), Table of Isotopes 1978 (green down triangles), Williams (pink stars), Sevier 1979 (turquoise asterisks) and G4AtomicShells (empty squares).

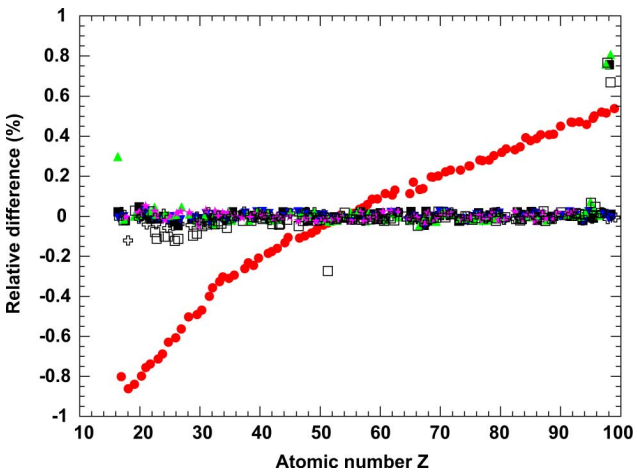

Fig. 13. KM_2 transition, relative difference between binding energies in various compilations and experimental data from [64] versus atomic number: EADL (red circles), Carlson (blue up triangles), Table of Isotopes 1996 (black squares), Table of Isotopes 1978 (green down triangles), Williams (pink stars), Sevier 1979 (turquoise asterisks) and G4AtomicShells (empty squares).

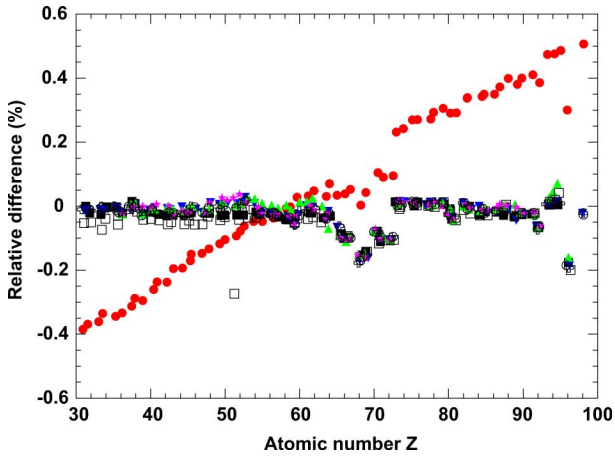

Fig. 14. KN_2 transition, relative difference between binding energies in various compilations and experimental data from [64] versus atomic number: EADL (red circles), Carlson (blue up triangles), Table of Isotopes 1996 (black squares), Table of Isotopes 1978 (green down triangles), Williams (pink stars), Sevier 1979 (turquoise asterisks) and G4AtomicShells (empty squares).

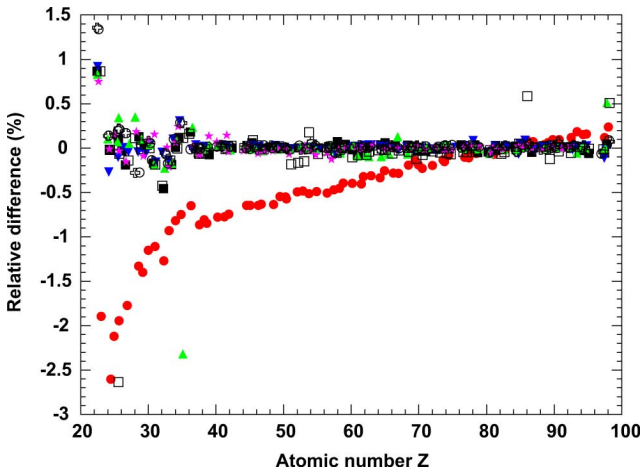

Fig. 15. L_1M_3 transition, relative difference between binding energies in various compilations and experimental data from [64] versus atomic number: EADL (red circles), Carlson (blue up triangles), Table of Isotopes 1996 (black squares), Table of Isotopes 1978 (green down triangles), Williams (pink stars), Sevier 1979 (turquoise asterisks) and G4AtomicShells (empty squares).

X-ray energies simulated by Geant4 are compatible with the experimental data with 0.1 significance for all transitions and all elements; the relative difference between simulated and experimental values is approximately 1–2% for most individual transitions. The present study is extended to binding energy compilations other than EADL.

A selection of representative plots of the relative difference between calculated X-ray energies and the experimental data of [64] is shown in Figs. 12–20; X-ray energies are calculated from the various compilations of binding energies. It is evident from the plots that the energies calculated by EADL appear less accurate than those based on the other compilations. Nevertheless, as already found in [65], the discrepancies of the energies deriving from EADL with respect to measurements are quite small (less than 2% in general).

Similarly to what has been discussed in the previous section, goodness-of-fit tests based on the empirical distribution function are not sensitive to such small differences: the hypothesis of compatibility between experimental data and X-ray energies based on EADL (the compilation that is evidently responsible for the largest discrepancies) is not rejected at 0.1 level of significance [65].

The χ^2 test has limited discriminant power as well, due to the small uncertainties of the experimental reference data in [64] (less than 0.1 eV for some transitions), which lead to the rejection of the null hypothesis of compatibility between calculated and experimental X-ray energies in a large number of test cases. It is hard to ascertain whether this result of the χ^2 test is due to underestimated uncertainties for some transitions and elements, or reflects a realistic conclusion that X-ray energies calculated from binding energy differences do not achieve the same accuracy by which X-ray energies are experimentally measured.

Similarly to what was described in the previous section, a t-test was applied to evaluate whether the distribution of dif-

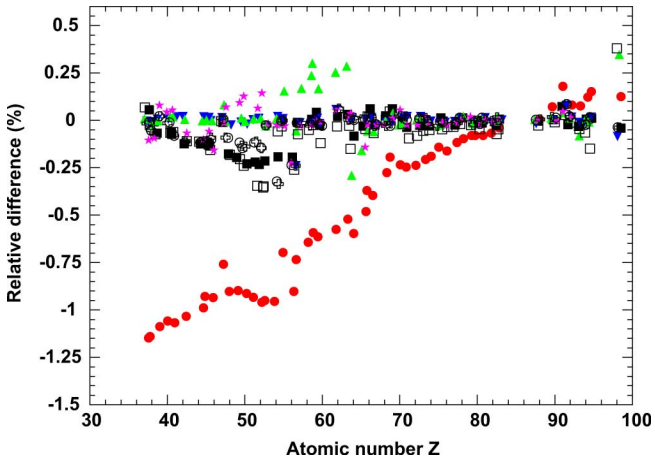

Fig. 16. L_3N_2 transition, relative difference between binding energies in various compilations and experimental data from [64] versus atomic number: EADL (red circles), Carlson (blue up triangles), Table of Isotopes 1996 (black squares), Table of Isotopes 1978 (green down triangles), Williams (pink stars), Sevier 1979 (turquoise asterisks) and G4AtomicShells (empty squares).

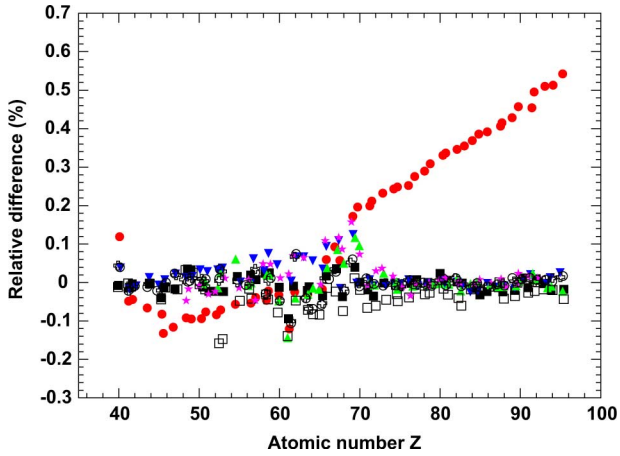

Fig. 18. L_2N_4 transition, relative difference between binding energies in various compilations and experimental data from [64] versus atomic number: EADL (red circles), Carlson (blue up triangles), Table of Isotopes 1996 (black squares), Table of Isotopes 1978 (green down triangles), Williams (pink stars), Sevier 1979 (turquoise asterisks) and G4AtomicShells (empty squares).

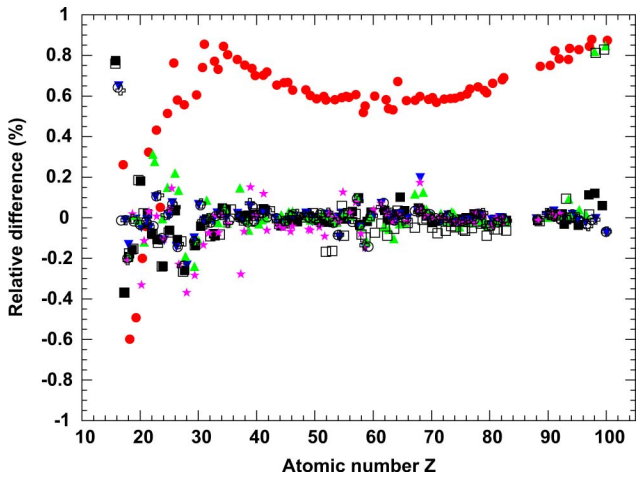

Fig. 17. L_2M_1 transition, relative difference between binding energies in various compilations and experimental data from [64] versus atomic number: EADL (red circles), Carlson (blue up triangles), Table of Isotopes 1996 (black squares), Table of Isotopes 1978 (green down triangles), Williams (pink stars), Sevier 1979 (turquoise asterisks) and G4AtomicShells (empty squares).

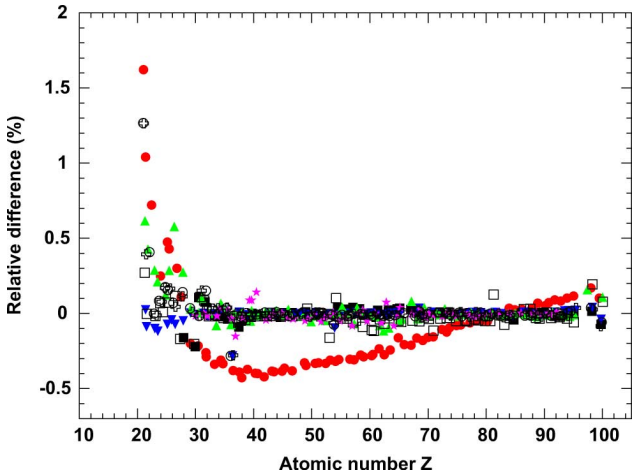

Fig. 19. L_3M_5 transition, relative difference between binding energies in various compilations and experimental data from [64] versus atomic number: EADL (red circles), Carlson (blue up triangles), Table of Isotopes 1996 (black squares), Table of Isotopes 1978 (green down triangles), Williams (pink stars), Sevier 1979 (turquoise asterisks) and G4AtomicShells (empty squares).

ferences between calculated and experimental X-ray energies is compatible with a true mean of zero. For each transition the t-test was performed over all the elements for which experimental values are reported in[64]; the fraction of test cases for each transition for which the hypothesis of compatibility is not rejected with 0.05 significance is listed in Table VI.

The largest number of test cases where the hypothesis of compatibility with null average difference is not rejected with 0.05 significance is achieved by the compilations of the 1996 Tables of Isotopes and Bearden and Burr's review (44 out of 48 test cases).

The hypothesis whether the compatibility of the other binding energy compilations with zero mean is equivalent to the one achieved by the 1996 Table of Isotopes and Bearden and Burr's review was tested by means of contingency tables. Contingency tables were built by counting in how many t-test cases the rejection of the null hypothesis occurs, or does not occur; these counts are respectively identified as "fail" or "pass". The results concerning K and L shells are summed to obtain a larger sample size. They were analyzed by means of Fisher's exact test [67], Pearson's χ^2 test (whenever the number of entries in each cell justifies the use of this test) and the χ^2 test with Yates continuity correction [69]. The contingency table concerning the comparison of EADL and the 1996 Table of Isotopes is reported in Table VII, along with the p-values of the three tests applied to it.

The hypothesis of equivalence with respect to the results of the t-test is rejected with 0.05 significance for EADL; it is not rejected for Carlson's, Sevier's and Williams' compilations. The outcome of the tests is controversial for the contingency table concerning the 1996 and 1978 editions of the Table of Isotopes: the p-values are 0.050 for Fisher's exact test, 0.039 for Person's χ^2 test and 0.075 for the χ^2 with Yates' continuity correction. The compatibility between EADL and the the 1996 Table of

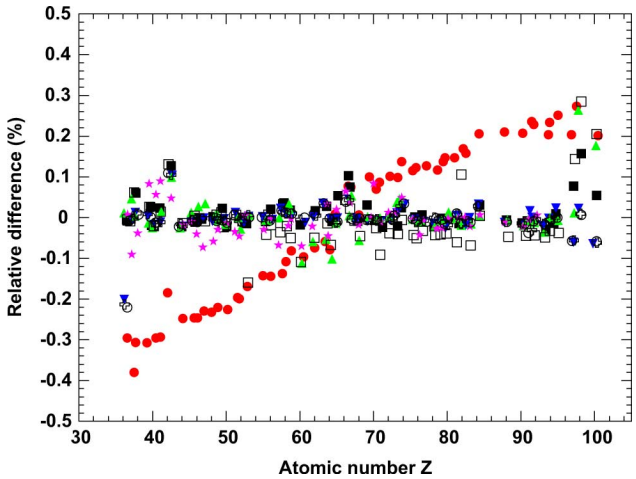

Fig. 20. L_3N_1 transition, relative difference between binding energies in various compilations and experimental data from [64] versus atomic number: EADL (red circles), Carlson (blue up triangles), Table of Isotopes 1996 (black squares), Table of Isotopes 1978 (green down triangles), Williams (pink stars), Sevier 1979 (turquoise asterisks) and G4AtomicShells (empty squares).

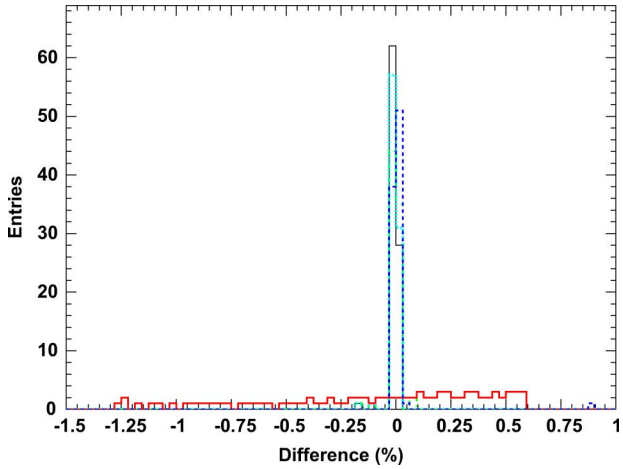

Fig. 21. KL_3 transition, relative difference between binding energies in various compilations and experimental data from [64]: EADL (thick solid red line), Carlson (dashed blue line), Table of Isotopes 1996 (thin solid black line), Williams (dash-dotted green line), Sevier 1979 (dotted turquoise line); the results of the other compilations considered in this study, which are not shown, exhibit a narrow distribution similar to the other compilations, except EADL.

TABLE VI
NUMBER OF TEST CASES COMPATIBLE AT 0.05 SIGNIFICANCE LEVEL WITH MEAN NULL DIFFERENCE BETWEEN CALCULATED AND EXPERIMENTAL X-RAY ENERGIES

Compilation	K	L_1	L_2	L_3	K+L	Fraction
Bearden and Burr	10	12	11	11	44	0.92 ± 0.04
Carlson	7	11	11	9	38	0.79 ± 0.06
EADL	8	4	1	3	16	0.33 ± 0.07
Sevier 1979	10	9	12	9	40	0.83 ± 0.05
ToI 1978	7	11	8	9	35	0.76 ± 0.06
ToI 1996	9	12	11	12	44	0.92 ± 0.04
Williams	8	12	11	9	40	0.85 ± 0.05

TABLE VII
CONTINGENCY WITH THE T-TEST: APPLIED TO X-RAY ENERGIES DERIVED FROM EADL AND FROM THE 1996 ISOTOPES

χ^2 test outcome	ToI 1996	EADL
Pass	44	16
Fail	4	32
p-value Fisher test	< 0.0001	
p-value Pearson χ^2	not applicable	
p-value Yates χ^2	< 0.0001	

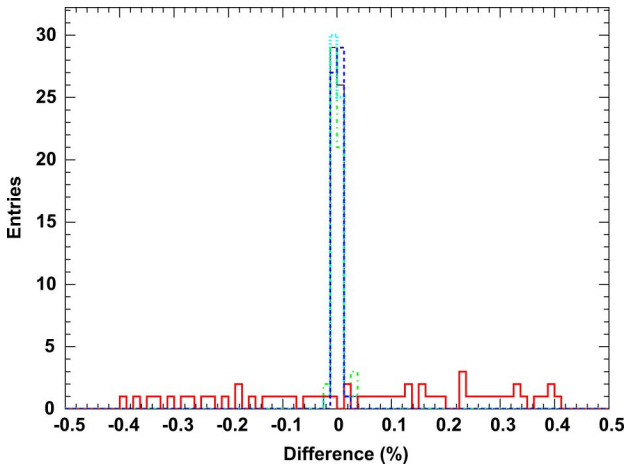

Fig. 22. kM_3 transition, relative difference between binding energies in various compilations and experimental data from [64]: EADL (thick solid red line), Carlson (dashed blue line), Table of Isotopes 1996 (thin solid black line), Williams (dash-dotted green line), Sevier 1979 (dotted turquoise line); the results of the other compilations considered in this study, which are not shown, exhibit a narrow distribution similar to the other compilations, except EADL.

Isotopes is excluded even if a looser 0.01 significance for the rejection of the null hypothesis is set both in the t-test and in the contingency tables.

The distribution of the difference between the X-ray energies calculated from binding energy tabulations and the experimental values of [64] is wider for EADL than for all the other compilations; this result can be appreciated in a few representative plots (Figs. 21–25).

The equivalence of the variance of the differences between calculated and experimental X-ray energies was estimated by means of the F-test. For each transition, the variance of the corresponding data sample was compared to the variance associated with the 1996 Table of Isotopes, which exhibits the narrowest distribution of differences between calculated and experimental X-ray energies. The hypothesis of equivalence of the variances under test was rejected if the p-value from the F-test was smaller than 0.01. The fraction of transitions for which the outcome of the F-test indicates that there is no significant difference in the respective variances is listed in Table VIII.

The results of the F-test are consistent With the qualitative appraisal of the accuracy of the distributions in Figs. 21–25. It is worthwhile to recall that the F-test is sensitive to the normality of the distributions to which is applied; although the differences between calculated and experimental data are expected to be normally distributed, the results reported in Table VIII may be affected by some details of the distributions subject to comparison.

The analysis of X-ray energies suggests that better accuracy in the reproduction of K and L transition energies can be achieved by binding energy compilations other than EADL. The original design of Geant4 atomic relaxation described in [66] would easily accommodate the improvement of the accuracy of the simulated energies through alternative binding

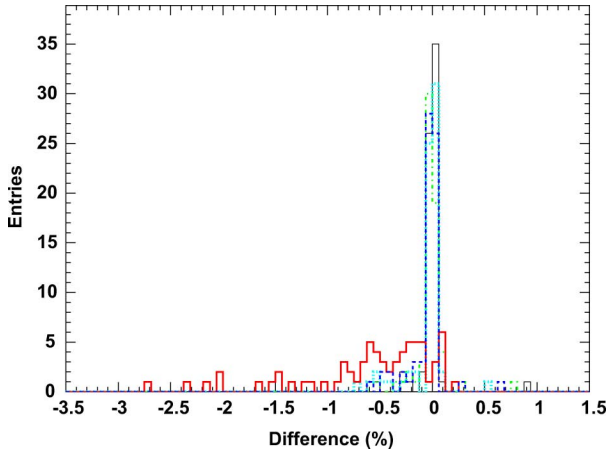

Fig. 23. L_1M_2 transition, relative difference between binding energies in various compilations and experimental data from [64]: EADL (thick solid red line), Carlson (dashed blue line), Table of Isotopes 1996 (thin solid black line), Williams (dash-dotted green line), Sevier 1979 (dotted turquoise line); the results of the other compilations considered in this study, which are not shown, exhibit a narrow distribution similar to the other compilations, except EADL.

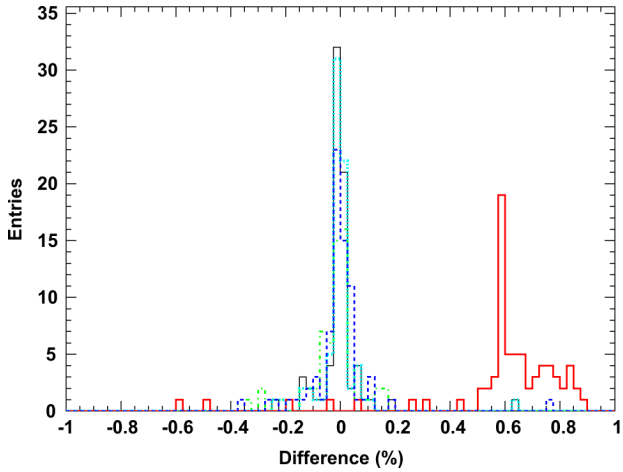

Fig. 24. L_2M_1 transition, relative difference between binding energies in various compilations and experimental data from [64]: EADL (thick solid red line), Carlson (dashed blue line), Table of Isotopes 1996 (thin solid black line), Williams (dash-dotted green line), Sevier 1979 (dotted turquoise line); the results of the other compilations considered in this study, which are not shown, exhibit a narrow distribution similar to the other compilations, except EADL.

energy options: the software implementation would handle the process of atomic relaxation transparently, if a different tabulation of binding energies is supplied as an external file.

VI. Effects on Ionization Cross Sections

Some analytical formulations of cross sections for the ionization of atoms by charged particle impact involve atomic binding energies. Two of these models are considered in this study to ascertain whether different binding energy compilations would produce significant differences in the cross section values: the Binary-Encounter-Bethe model (BEB) [70] for electron impact ionization and the ECPSSR (Energy Loss Coulomb Repulsion Perturbed Stationary State Relativistic) model [71] for proton impact ionization. For both models the effects on the accuracy of the cross section calculations are quantitatively estimated through a comparison with experimental data.

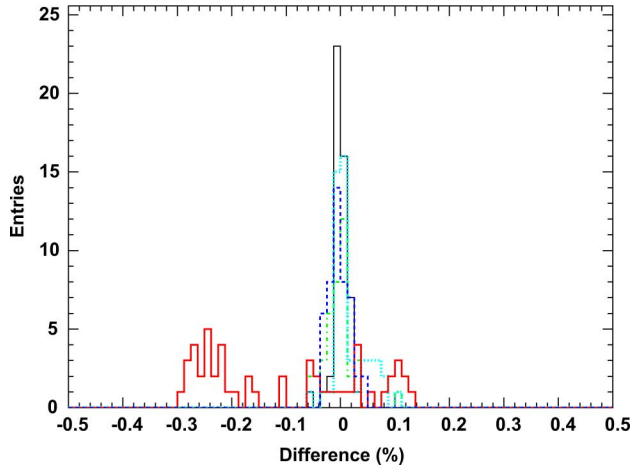

Fig. 25. LN_3 transition, relative difference between binding energies in various compilations and experimental data from [64]: EADL (thick solid red line), Carlson (dashed blue line), Table of Isotopes 1996 (thin solid black line), Williams (dash-dotted green line), Sevier 1979 (dotted turquoise line); the results of the other compilations considered in this study, which are not shown, exhibit a narrow distribution similar to the other compilations, except EADL.

TABLE VIII
Fraction of K and L Transitions for Which the Variance of the Difference Between Calculated and Experimental X-ray Energies is Equivalent to the Variance Associated With the 1996 Isotopes

Compilation	Fraction of transitions
Bearden and Burr	0.60 ± 0.07
Carlson	0.69 ± 0.07
EADL	0.25 ± 0.06
Sevier 1979	0.79 ± 0.06
ToI 1978	0.65 ± 0.07
Williams	0.70 ± 0.07

A. Electron Impact Ionization Cross Sections

Two models of electron impact cross sections, the Binary-Encounter-Bethe [70] model and the Deutsch-Märk model [72], have been designed, implemented and validated in view of extending and improving Geant4 simulation capabilities in the energy range below 1 keV. Their features, verification and validation are briefly summarized in [73], [74] and extensively documented in a dedicated paper [75]. The first software development cycle has been focused on modeling total ionization cross sections; the validation process and the analysis of the effect of atomic binding energies concern these calculations, although the BEB model has the capability of calculating cross sections for the ionisation of individual shells. The BEB cross section for the ionization of subshell i is given by

$$\sigma_i = \frac{S}{t + \frac{(u+1)}{n}} \left[\frac{\log(t)}{2} \left(1 - \frac{1}{t^2} \right) + 1 - \frac{1}{t} - \frac{\log(t)}{t+1} \right] \quad (1)$$

where

$$t = \frac{T}{B},\ u = \frac{U}{B},\ S = 4\pi a_0^2 N \left(\frac{R}{B} \right)^2. \quad (2)$$

In the above equations B is the electron binding energy, N is the the occupation number, T is the incident electron energy, U is the average electron kinetic energy, t and u are normalized incident and kinetic energies, n is the principal quantum number (only taken into account when larger than 2), a_0 is the

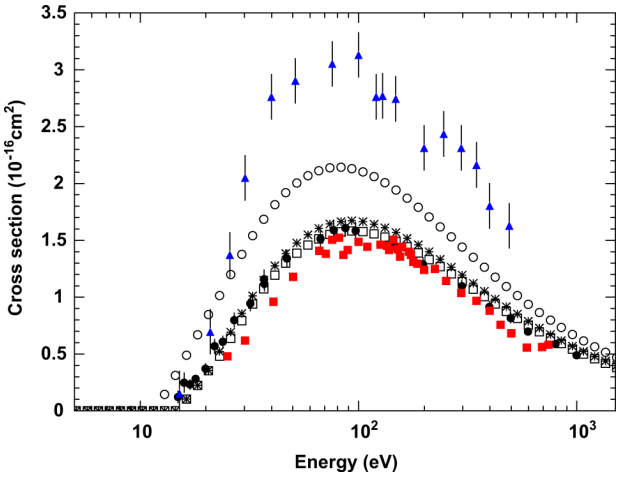

Fig. 26. BEB electron impact ionization cross section, Z = 7: BEB model with EADL binding energies for all shells (empty circles), BEB model with EADL binding energies except for ionization energies replaced by NIST values (empty squares), BEB model with Lotz binding energies (asterisks) and experimental data from [103] (black circles), [104] (red squares) and [105] (blue triangles).

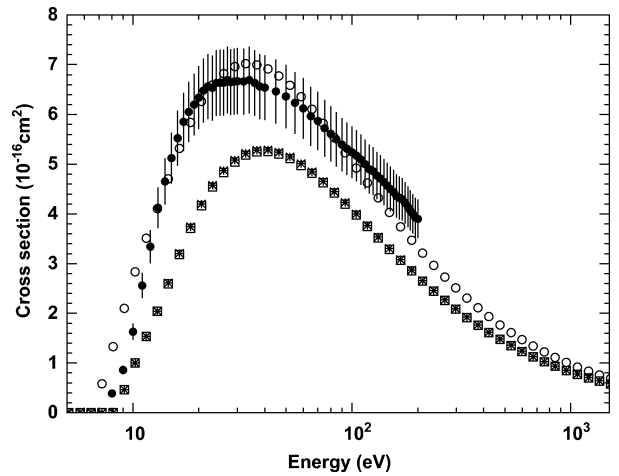

Fig. 27. BEB electron impact ionization cross section, Z = 14; BEB model with EADL binding energies for all shells (empty circles), BEB model with EADL binding energies except for ionization energies replaced by NIST values (empty squares), BEB model with Lotz binding energies (asterisks) and experimental data from [118] (black circles).

TABLE IX
TEST CASES IN WHICH THE HYPOTHESIS OF COMPATIBILITY OF BEB CROSS SECTIONS BASED ON LOTZ AND MODIFIED EADL BINDING ENERGIES IS NOT REJECTED

Test	Fraction (E < 100 eV)	Fraction (E > 100 eV)
Kolmogorov-Smirnov	0.91 ± 0.05	1.00 − 0.02
Anderson-Darling	0.97 ± 0.03	1.00 − 0.02
Cramer-von Mises	0.97 ± 0.03	1.00 − 0.02

Bohr radius and R is the Rydberg constant. The sum over all the subshells i of an atom gives the total (counting) cross section; in practice, only the valence shell and a few outer subshells contribute significantly to determine the cross section value.

The original BEB cross sections [70] used binding energy values calculated by the authors of the model. Only a few of those values are documented in [70]; they were utilized in the software verification process to assess the correctness of the implementation, but such a small set is inadequate for using the model in a general purpose simulation system, which must be able to calculate cross sections for any target atoms. The BEB model developed for use with Geant4 utilizes a full set of binding energies and provides the option of accessing alternative compilations.

TABLE X
TEST CASES IN WHICH THE HYPOTHESIS OF COMPATIBILITY OF BEB CROSS SECTIONS BASED ON EADL AND MODIFIED EADL IS NOT REJECTED

Test	Fraction (E < 100 eV)	Fraction (E > 100 eV)
Kolmogorov-Smirnov	0.70 ± 0.05	0.98 ± 0.02
Anderson-Darling	0.83 ± 0.04	0.98 ± 0.02
Cramer-von Mises	0.95 ± 0.02	1.00 − 0.02

The analysis addressed two issues: the sensitivity of cross sections to the values of the binding energies used in the calculation, and the evaluation of the accuracy with respect to experimental data.

Two examples of the effects of different binding energies on the calculated cross sections are shown in Figs. 26 and 27. They illustrate three options of binding energies: Lotz's compilation, which is also used by the Deutsch-Märk model, EADL data for all shells and EADL with ionization potentials replaced by NIST values [25] (identified in the following as "modified EADL"). Lotz's compilation is identical to Carlson's apart from a few exceptions; according to the analysis in Section IV-C, Carlson's compilation appears the most accurate with respect to NIST ionization potentials, while EADL exhibits the largest differences with respect to other compilations in both inner and outer-shell binding energies. Significant differences are visible in the cross sections, when different ionization energies are used in the calculation, while different inner-shell binding energies appear to have relatively small effects.

The effect of these three options, which can be considered as extreme alternatives in the BEB calculation, has been quantified through a statistical analysis.

First, cross sections calculated with different binding energies were compared via goodness-of-fit tests; the test concerned all elements with atomic number between 1 and 92, and incident electron energies from 1 eV to 10 keV, divided in two ranges: those up to 100 eV, and those above. The results of the comparisons are summarized in Tables IX and X. The Kolmogorov-Smirnov test appears the most sensitive to differences in the cross sections deriving from the considered binding energy options. The hypothesis of compatibility between cross sections calculated with Lotz's binding energies and with modified EADL is rejected with 0.05 significance only for a few heavy elements (with Z > 80) in the lower energy range (below 100 eV): this result indicate that total ionization cross sections are marginally affected by inner-shell binding energies. The hypothesis of compatibility between the cross sections based on EADL and modified EADL is rejected in a larger number of test cases, especially in the lower energy range: this result shows that the cross sections are sensitive to the values of the ionization potential.

The following analysis evaluated whether different ionization potentials would significantly affect the accuracy of the calculated cross sections with respect to experimental data.

TABLE XI
TEST CASES FOR WHICH THE HYPOTHESIS OF COMPATIBILITY OF BEB CROSS SECTIONS WITH EXPERIMENTAL DATA IS REJECTED, OR NOT REJECTED, WITH 0.05 SIGNIFICANCE

Energy	EADL			Modified EADL		
(eV)	Pass	Fail	Pass Fraction	Pass	Fail	Pass Fraction
< 20	67	40	0.63±0.05	79	28	0.74±0.04
20-50	61	68	0.47±0.04	81	48	0.63±0.04
50-100	40	84	0.32±0.04	49	75	0.40±0.04
100-250	47	80	0.37±0.04	56	71	0.44±0.04
250-1000	45	31	0.59±0.06	47	29	0.62±0.06
>1000	14	11	0.56±0.10	14	11	0.56±0.10

The effects of different ionization energies on the accuracy of the calculation are not straightforward to ascertain from a qualitative appraisal of the data: in fact, within the data sample one can identify test cases where either configuration—with NIST values or with EADL original values—appears to better reproduce the experimental data as shown, for instance, in Figs. 26 and 27. Therefore a statistical analysis was performed, examining the compatibility with experiment of two sets of BEB cross sections, which use respectively EADL binding energies for all shells, or the modified EADL with NIST ionization potentials. The two sets of cross sections were compared to the same experimental measurements [76]–[165], consisting of more than 150 individual data sets and concerning more than 50 elements. The comparison with experimental data exploits goodness-of-fit tests (Kolmogorov-Smirnov, Anderson-Darling, Cramer-von Mises and χ^2); their significance was set to 0.05. The test was articulated over five distinct energy ranges below 1 keV to appraise in detail the accuracy of the calculated cross sections.

The number of test cases for which the null hypothesis of compatibility between calculated and measured cross sections is rejected, or not rejected, is reported in Table XI for the two examined binding energy options. Below 1 keV the hypothesis of compatibility with experimental data is always rejected in a smaller number of test cases when the cross section calculation utilizes NIST ionization energies instead of EADL original ones. No difference is observed above 1 keV.

The analysis by means of contingency tables does not reject the hypothesis of equivalence between the two cross section categories at reproducing experimental data in any of the considered energy ranges. Nevertheless, the probability that the better performance associated with NIST ionization energies in all five trials could be due to chance only is 0.03.

B. Proton Impact Ionization Cross Sections

A similar study was performed on proton ionization cross sections. Several cross section models for the computation of inner-shell ionization by proton and α particle impact have been released in Geant4 version 9.4 [40]; they include calculations based on the plane wave Born approximation (PWBA) [166], the ECPSSR (Energy-loss Coulomb Perturbed Stationary State Relativistic) model [71] in a number of variants and a collection of empirical models, deriving from fits to experimental data. The PWBA and ECPSSR cross sections (in all their variants) exploit tabulations produced by the ISICS (Inner-Shell Ionization Cross Sections) code [41] for K, L and M shells.

The formulation of the PWBA and ECPSSR cross sections involves atomic binding energies. For a given shell the PWBA cross section is given by

$$\sigma_{\mathrm{PWBA}} = \sigma_0 \theta^{-1} F\left(\frac{\eta}{\theta}, \theta\right) \tag{3}$$

where

$$\sigma_0 = 8\pi a_0^2 \left(\frac{Z_1^2}{Z_2^4}\right) \tag{4}$$

a_0 is the Bohr radius, Z_1 is the projectile atomic number, Z_2 is the effective atomic number of the target atom, F is the reduced universal cross section, with the reduced atomic electron binding energy θ and reduced projectile energy η given by

$$\theta = 2n^2 \frac{U_2}{Z_2^2} \tag{5}$$

and

$$\eta = 2\frac{E_1}{M_1 Z_2^2} \tag{6}$$

respectively. In (5) and (6) E, M and U represent the energy, mass and atomic binding energy. In the above formulae the indices 1 and 2 refer respectively to the projectile and the target. The analytical formulation of the reduced universal cross section F can be found in [41]; it involves the reduced atomic electron binding energy. The ECPSSR cross section for a given shell is expressed in terms of the PWBA value

$$\sigma_{\mathrm{ECPSSR}} = C_B^E(dq_0{}^B\zeta)\sigma_{\mathrm{PWBA}}\left(\frac{m_R\left(\frac{\xi}{\zeta}\right)\eta}{(\zeta\theta)^2}, \zeta\theta\right) \tag{7}$$

where C_E^B is the Coulomb deflection correction, ζ is the correction factor for binding energy and polarization effects, m_R is the relativistic correction, q_0 is the minimum momentum transfer and

$$\xi = v_1 \frac{Z_2}{U_2} \tag{8}$$

v_1 being the projectile velocity.

The PWBA and ECPSSR cross section tabulations distributed with the Geant4 code were produced with the ISICS 2008 version, which uses the Bearden and Burr binding energies. Recent updates to ISICS [46] offer the option of using Williams' compilation of binding energies as alternative values to the default Bearden and Burr's ones; a further evolution of ISICS [167] lets the user specify an arbitrary source of atomic binding energies, thus providing access to any of the options analyzed in this paper. This version, which was used to produce the data for this paper, involves new implementations of some parts of the ISICS code, which contribute to the numerical correctness and computational robustness of the software. The new features and verification of this new version of ISICS are documented in [167]. The experimental validation of cross sections generated by this new version of ISICS produces consistent results with those reported in [40], when the two code versions are run in the same configuration.

Cross sections calculated by ISICS 2011 version using different binding energy compilations exhibit differences; some

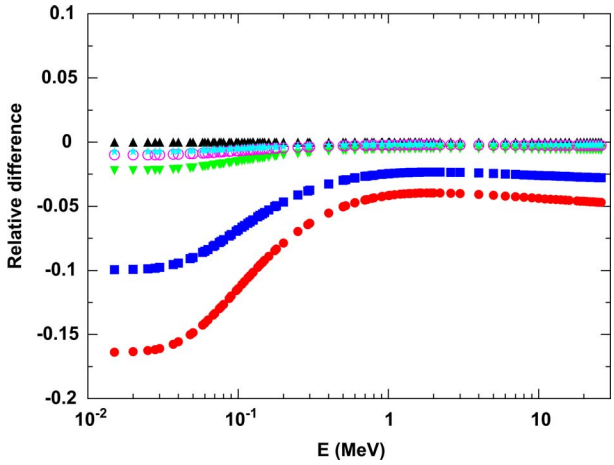

Fig. 28. Carbon K shell ionization cross sections by proton impact calculated by the ECPSSR model with different binding energies: the plot shows the relative difference with respect to the values calculated with Bearden and Burr's binding energies used by default by ISICS; the symbols identify cross sections calculated with EADL (red circles), Carlson (blue squares), 1996 Table of Isotopes (black up triangles), 1978 Table of Isotopes (green down triangles), Williams (pink empty circles) and Sevier 1979 (turquoise stars) binding energies. Some symbols are not visible in the plot due to the close values of some cross sections.

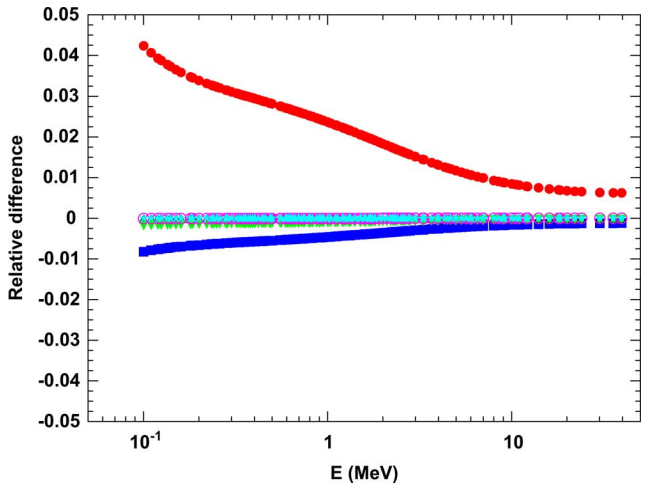

Fig. 29. Copper K shell ionization cross sections by proton impact calculated by the ECPSSR model with different binding energies: the plot shows the relative difference with respect to the values calculated with Bearden and Burr's binding energies used by default by ISICS; the symbols identify cross sections calculated with EADL (red circles), Carlson (blue squares), 1996 Table of Isotopes (black up triangles), 1978 Table of Isotopes (green down triangles), Williams (pink empty circles) and Sevier 1979 (turquoise stars) binding energies. Some symbols are not visible in the plot due to the close values of some cross sections.

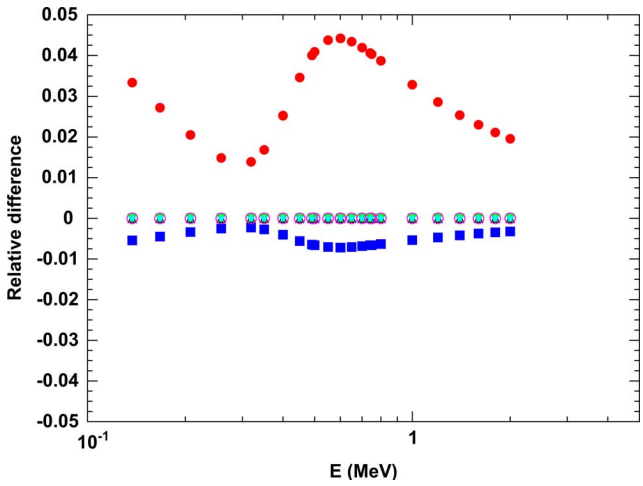

Fig. 30. Cadmium L_1 shell ionization cross sections by proton impact calculated by the ECPSSR model with different binding energies: the plot shows the relative difference with respect to the values calculated with Bearden and Burr's binding energies used by default by ISICS; the symbols identify cross sections calculated with EADL (red circles), Carlson (blue squares), 1996 Table of Isotopes (black up triangles), 1978 Table of Isotopes (green down triangles), Williams (pink empty circles) and Sevier 1979 (turquoise stars) binding energies. Some symbols are not visible in the plot due to the close values of some cross sections.

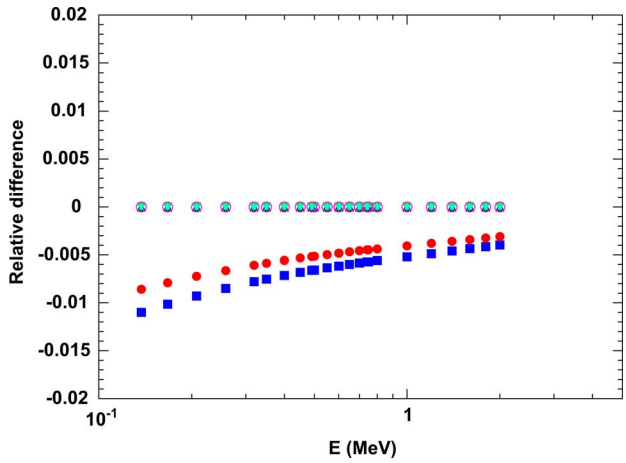

Fig. 31. Cadmium L_2 shell ionization cross sections by proton impact calculated by the ECPSSR model with different binding energies: the plot shows the relative difference with respect to the values calculated with Bearden and Burr's binding energies used by ISICS; the symbols identify cross sections calculated with EADL (red circles), Carlson (blue squares), 1996 Table of Isotopes (black up triangles), 1978 Table of Isotopes (green down triangles), Williams (pink empty circles) and Sevier 1979 (turquoise stars) binding energies. Some symbols are not visible in the plot due to the close values of some cross sections.

examples, concerning K and L shells, are shown in Figs. 28–32. The differences appear larger for light elements and K shell.

The effects of different binding energies on the accuracy of proton ionization cross sections have been evaluated by comparing values based on various binding energy collections with experimental data for K and L shells. The experimental data derive from the reviews by Paul and Sacher [168], Sokhi and Crumpton [169] and Orlic *et al.* [170]; the comparison process adopts the same strategy described in [40] for the validation of the cross section models available in Geant4. For each element, the compatibility between calculated and experimental cross sections is evaluated by means of the χ^2 test; the significance of the test for the rejection of the null hypothesis of equivalence of the compared distributions is set to 0.05.

The analysis of the sensitivity to electron binding energies is reported here for plain ECPSSR cross sections. The fraction of tested elements for which K shell cross sections calculated with various binding energies are compatible with experimental data is listed in Table XII: with the exception of EADL, all binding energy compilations appear to produce equivalently accurate cross sections. The use of EADL binding energies results in fewer test cases that are compatible with measurements; the hypothesis of equivalent accuracy of cross sections based

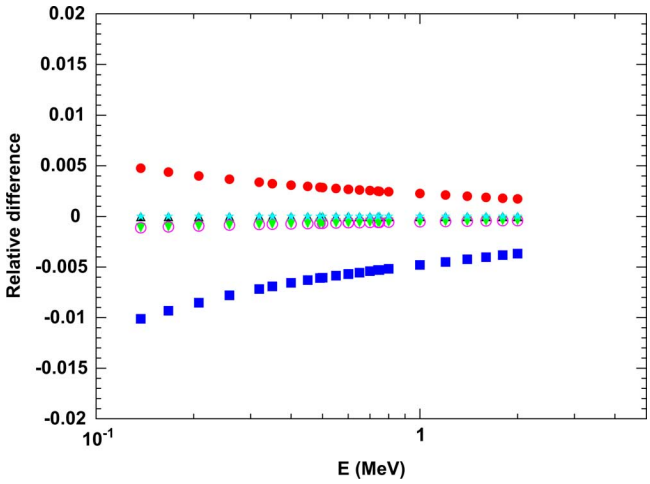

Fig. 32. Cadmium L_3 shell ionization cross sections by proton impact calculated by the ECPSSR model with different binding energies: the plot shows the relative difference with respect to the values calculated with Bearden and Burr's binding energies used by default by ISICS; the symbols identify cross sections calculated with EADL (red circles), Carlson (blue squares), 1996 Table of Isotopes (black up triangles), 1978 Table of Isotopes (green down triangles), Williams (pink empty circles) and Sevier 1979 (turquoise stars) binding energies. Some symbols are not visible in the plot due to the close values of some cross sections.

TABLE XII
FRACTION OF TESTED ELEMENTS FOR WHICH ECPSSR K SHELL CROSS SECTIONS ARE COMPATIBLE WITH EXPERIMENTAL DATA

Compilation	Fraction
Bearden and Burr	0.76 ± 0.05
Carlson	0.76 ± 0.05
EADL	0.58 ± 0.06
Sevier 1979	0.76 ± 0.05
ToI 1978	0.78 ± 0.05
ToI 1996	0.76 ± 0.05
Williams	0.78 ± 0.05

TABLE XIII
CONTINGENCY ESTIMATE THE EQUIVALENT ACCURACY OF ECPSSR K SHELL CROSS SECTIONS USING EADL AND BEARDEN AND BURR'S BINDING ENERGIES

χ^2 test outcome	Bearden and Burr	EADL
Pass	51	39
Fail	16	28
p-value Fisher test	0.042	
p-value Pearson χ^2	0.027	
p-value Yates χ^2	0.043	

on EADL with those based on other compilations is rejected with 0.05 significance for all the alternative binding energies. As an example, the contingency table comparing the compatibility with experimental data of cross sections based on EADL and Bearden and Burr binding energies is reported in Table XIII.

The differences of cross sections associated with binding energy compilations are smaller for L shell than for K shell, as one can qualitatively observe in two examples, concerning cadmium and tungsten, shown in Figs. 30–35. The comparison of L shell cross sections with experimental data does not identify any significant differences associated with the use of different binding energies; the fraction of tested elements for which L shell cross sections calculated with various binding energies are compatible with experimental data is listed in Table XIV.

TABLE XIV
FRACTION OF TESTED ELEMENTS FOR WHICH ECPSSR L SHELL CROSS SECTIONS ARE COMPATIBLE WITH EXPERIMENTAL DATA

Compilation	Fraction, L_1	Fraction, L_2	Fraction, L_3
Bearden and Burr	0.68 ± 0.09	0.68 ± 0.09	0.89 ± 0.06
Carlson	0.68 ± 0.09	0.68 ± 0.09	0.86 ± 0.07
EADL	0.64 ± 0.09	0.64 ± 0.09	0.89 ± 0.06
Sevier 1979	0.68 ± 0.09	0.68 ± 0.09	0.89 ± 0.06
ToI 1978	0.68 ± 0.09	0.68 ± 0.09	0.89 ± 0.06
ToI 1996	0.68 ± 0.09	0.68 ± 0.09	0.89 ± 0.06
Williams	0.68 ± 0.09	0.68 ± 0.09	0.89 ± 0.06

The scarcity of experimental measurements prevents a similar analysis on the effect of binding energies on M shell ionization cross sections.

Based on this analysis, the accuracy of proton ionization cross sections appears statistically equivalent for all binding energy options but EADL.

VII. EFFECTS ON COMPTON SCATTERING

Doppler broadening of photon energy spectra arises from Compton scattering between photons and moving electrons bound to atoms of the target medium. Algorithms to account for Doppler broadening are implemented in widely used Monte Carlo systems: those included in EGS [171], MCNP [172] and Geant4 [173] are based on the method described in [171]; the algorithm implemented in Penelope produces equivalent results [173].

A test was performed to ascertain if different binding energy compilations would affect the calculated energy distributions of Compton scattering generated in the simulation. The test concerned a few target materials relevant to Compton telescopes [174], silicon, germanium and xenon, which are characterized by different experimental resolutions related to the effects of Doppler broadening. For this investigation, the original implementation of Compton scattering with Doppler broadening in Geant4 and associated unit test [173] was used. The analysis compared the spectra deriving from two sets of binding energies: those used in the simulation, which derive from EADL, and Carlson's compilation. The latter was chosen as its binding energies for the considered elements exhibit the largest difference with respect to EADL ones among the various examined compilations.

No significant effect was visible in the spectra of the scattered photons as a result of simulations using different binding energy compilations. An example is illustrated in Fig. 36, which shows the energy spectrum of photons between 89° and 91° resulting from Compton scattering of 40 keV photons orthogonally impinging onto a silicon target.

Pearson's χ^2 test confirms the equivalence of the Doppler broadened photon spectra based on EADL and Carlson's binding energies; the p-value resulting from this test is 1 for all the three target materials.

Therefore, based on this investigation, one can conclude that the choice of binding energy compilation is not critical for the simulation of Compton scattering accounting for Doppler broadening.

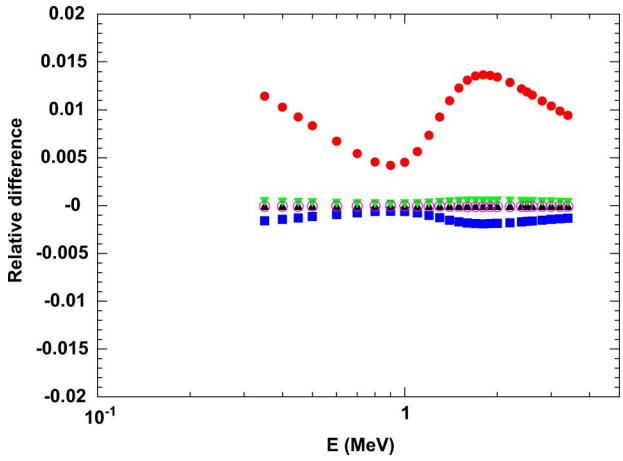

Fig. 33. Tungsten L_1 shell ionization cross sections by proton impact calculated by the ECPSSR model with different binding energies: the plot shows the relative difference with respect to the values calculated with Bearden and Burr's binding energies used by default by ISICS; the symbols identify cross sections calculated with EADL (red circles), Carlson (blue squares), 1996 Table of Isotopes (black up triangles), 1978 Table of Isotopes (green down triangles), Williams (pink empty circles) and Sevier 1979 (turquoise stars) binding energies. Some symbols are not visible in the plot due to the close values of some cross sections.

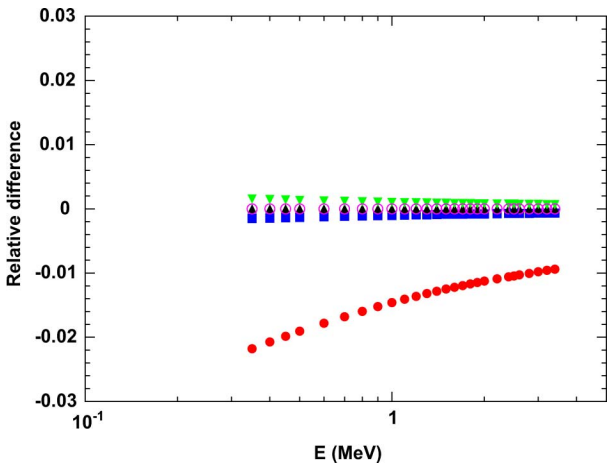

Fig. 34. Tungsten L_2 shell ionization cross sections by proton impact calculated by the ECPSSR model with different binding energies: the plot shows the relative difference with respect to the values calculated with Bearden and Burr's binding energies used by default by ISICS; the symbols identify cross sections calculated with EADL (red circles), Carlson (blue squares), 1996 Table of Isotopes (black up triangles), 1978 Table of Isotopes (green down triangles), Williams (pink empty circles) and Sevier 1979 (turquoise stars) binding energies. Some symbols are not visible in the plot due to the close values of some cross sections.

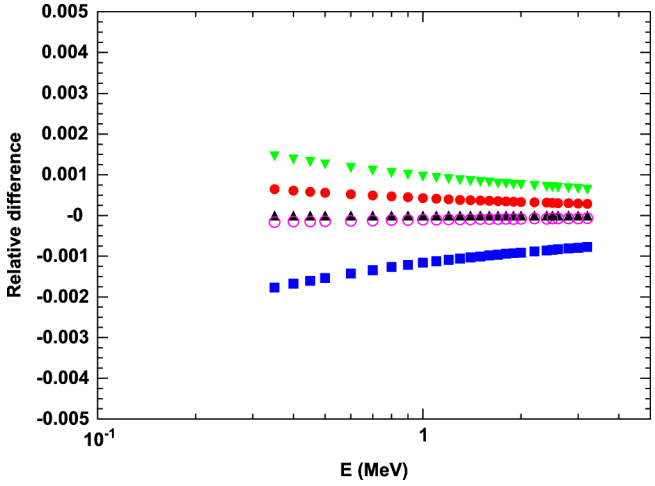

Fig. 35. Tungsten L_3 shell ionization cross sections by proton impact calculated by the ECPSSR model with different binding energies: the plot shows the relative difference with respect to the values calculated with Bearden and Burr's binding energies used by default by ISICS; the symbols identify cross sections calculated with EADL (red circles), Carlson (blue squares), 1996 Table of Isotopes (black up triangles), 1978 Table of Isotopes (green down triangles), Williams (pink empty circles) and Sevier 1979 (turquoise stars) binding energies. Some symbols are not visible in the plot due to the close values of some cross sections.

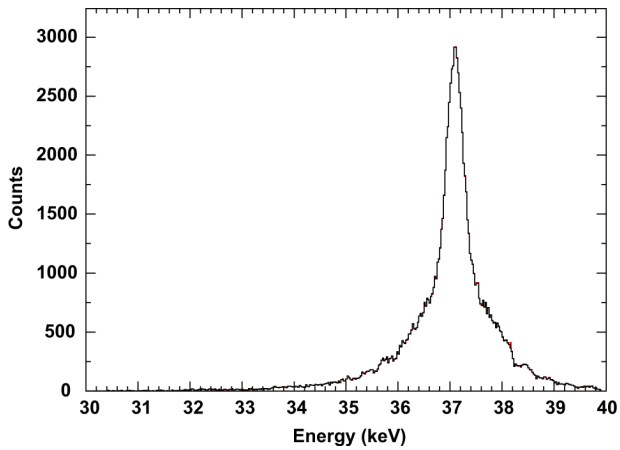

Fig. 36. Energy distribution of photons between 89° and 91° resulting from Compton scattering of 40 keV photons orthogonally impinging onto a silicon target, obtained using EADL (red) and Carlson's (black) binding energies in the simulation. The two histograms associated with either binding energy options are practically indistinguishable.

VIII. Merged Compilations

The collection of binding energies in Geant4's *G4AtomicShells* class has been assembled specifically for Geant4, merging data from Carlson's compilation with others from the 73rd edition of the CRC Handbook of Chemistry and Physics [33]. The origin of the data for each element and shell is documented in the form of comments in the code implementation. The authors of this paper could not retrieve a copy of the latter reference, which has been superseded by more recent editions (the most recent one at the time of writing this paper is the 91st edition); nevertheless, most of the values identified in the comments to the code as originating from [33] appear consistent with those published in the most recent version of the Handbook, which includes Williams' compilation. A few values in *G4AtomicShells*, however, are consistent with neither Carlson's nor Williams' compilations.

The two sources, Carlson's and Williams' compilations, report binding energies based on different reference levels: the vacuum level for Carlson's data and the Fermi level for Williams' data. Data referring to different reference levels are associated with shells of the same element in *G4AtomicShells*. The inconsistency of the data in the *G4AtomicShells* class may generate systematic effects in physics observables; some examples are illustrated in Figs. 37 and 38. These plots show the differences between X-ray energies calculated from

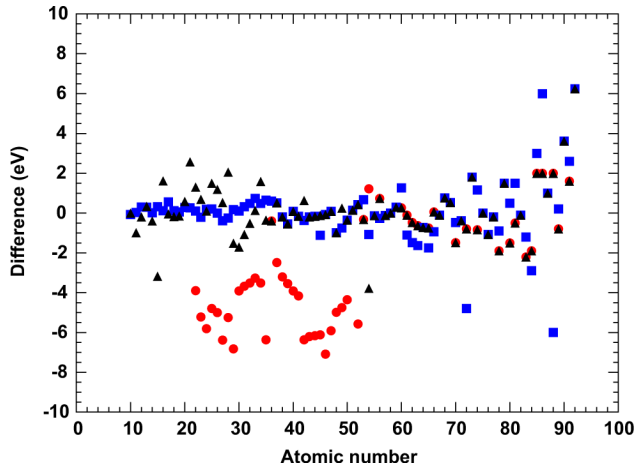

Fig. 37. KL_3 transition, difference between X-ray energies calculated from binding energies and experimental data from [64] versus atomic number: binding energies from *G4AtomicShells* (red circles), from Carlson (blue squares) and Williams (black triangles).

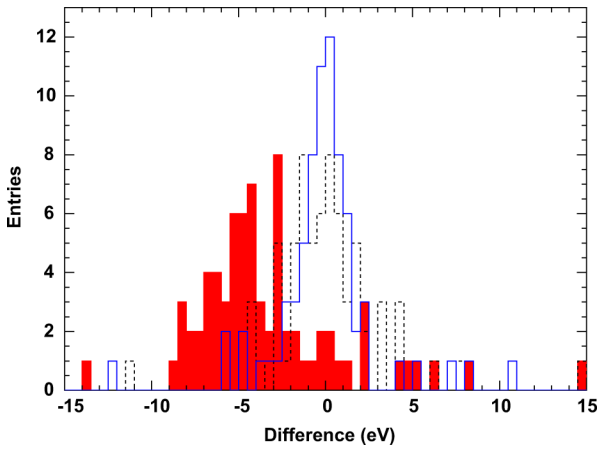

Fig. 38. KM_2 transition, difference between X-ray energies calculated from binding energies and experimental data from [64]: binding energies from *G4AtomicShells* (red shaded histogram), Carlson (blue solid line histogram) and Williams (black dashed line histogram).

G4AtomicShells binding energies and the experimental data of Deslattes *et al.* [64], along with X-ray energies calculated from Carlson's and Williams' compilations: the X-ray energies based on G4AtomicShells exhibit some systematic shifts with respect to the experimental data, while the X-ray energies based on Carlson's and Williams' compilations do not appear affected by such systematic discrepancies with measurements. The systematic effect is so large, that statistical tests appear redundant to identify its occurrence.

IX. Comments About Basic Assumptions in Monte Carlo Particle Transport

It is worthwhile to remind the reader that, as stated in Section III, the study documented in this paper is driven by the pragmatic objective of identifying one or more optimal options, among the atomic binding energy compilations used by general-purpose Monte Carlo systems for particle transport, for use in experimental applications of these codes. The purpose of this paper is not to accurately describe the electronic energy levels in materials in general terms, but only in terms that are consistent with, and usable in the transport scheme adopted by current general purpose Monte Carlo systems. Evaluations of molecular binding or crystal lattice effects are not within the scope of this paper.

As it is highlighted in the title, this paper deals with atomic electron binding energies. This subject of investigation is consistent with the assumption governing particle transport in all general purpose Monte Carlo codes: particles are assumed to interact with free atoms of the medium. This condition is assumed to be satisfied in the whole course of the simulation, also when interactions with crystals are concerned. A consequence of this assumption is that the models of electromagnetic processes encompassed in general purpose Monte Carlo codes and the physics parameters involved in their formulation, such as electron binding energies, pertain to the atomic domain.

In general purpose Monte Carlo systems this discrete transport scheme is complemented by the calculation of continuous energy loss, concerning charged particle interactions affected by infrared divergence. Continuous energy losses are due to soft interactions with the atomic electrons (excitation and ionization loss) and to the emission of soft Bremsstrahlung photons. Parameters pertaining to compounds, such as mean ionization potentials and stopping powers, appear in condensed transport calculations; however, for the very nature of the condensed transport scheme, electron energy levels are not directly involved. Moreover, in Monte Carlo codes the material parameters involved in these calculations are usually derived from published reference tabulations, rather than calculated on-the-fly in the course of the simulation execution.

In the independent atom scheme adopted by general purpose Monte Carlo codes, models describing particle interactions with the medium are extended to molecules by means of the additivity approximation, which consists of approximating the molecular cross section for a process by the sum of the atomic cross sections of all the atoms in the molecule. The adoption of this scheme affects the whole formulation of electromagnetic processes in Monte Carlo transport codes: not only the calculation of cross sections, but also the generation of the associated final state.

The conceptual assumptions in particle transport determine the level of detail to which material properties are described in the simulation. This scheme, where discrete electromagnetic interactions of particles are assumed to occur only with atoms, involves atomic parameters only. In other words, only atomic electron binding energies are currently used, and are usable, in general purpose Monte Carlo systems for particle transport, while molecular binding energies do not appear in any implementation of physics models in these codes, nor could be usable in current systems.

For these reasons, the analysis documented in this paper is focused on the optimization of atomic electron binding energies, while it is not concerned with electronic energy levels in materials in more general terms. In this respect, it is not important to observe that, for instance, the ionization energy of atomic nitrogen is 14.5341 eV [25], while that of molecular

TABLE XV
OVERVIEW OF TEST CASES

Test case	Statistical tests	Best performance	Other suitable options	Worst performance
Reference binding energies (Powell)	t-test, F-test	Williams	Sevier 1979, Bearden and Burr	-
Reference binding energies (NIST)	t-test, F-test	Williams	Sevier 1979, Bearden and Burr	Carlson, EADL
Reference ionization energies (NIST)	Goodness-of-Fit	Carlson, Sevier 1979, ToI 1996	-	EADL
Reference X-ray energies	t-test, F-test	ToI 1996, Bearden and Burr	Williams, Sevier 1979	EADL
Total electron ionization cross sections	Goodness-of-Fit	Carlson, Lotz	Not enquired	EADL
K-shell proton ionization cross sections	Goodness-of-Fit	All but EADL	-	EADL
L-shell proton ionization cross sections	Goodness-of-Fit	Any	-	-
Compton scattering	Pearson's χ^2	Any	-	-

nitrogen is 15.5808 eV [18], since all physics models for particle interactions with nitrogen in current general purpose Monte Carlo systems assume that interactions occur with atomic nitrogen only, given that interactions with nitrogen molecules are treated as interactions with atomic nitrogen based on the above mentioned additivity approximation. Since particle interaction models using molecular binding energies do not exist in current codes, one cannot evaluate quantitatively to what extent the difference between physics models using atomic binding energies in the independent atom approximation and hypothetical models using molecular binding energies exempt from that approximation in particle transport would affect physics observables generated by the simulation. One can only remark that, for instance, electron impact ionization cross sections for nitrogen, shown in Fig. 26 are consistent with experimental measurements when they are calculated with optimal choices of atomic electron binding energies.

In simulation practice, the lower limit of validity of the independent atom assumption is conventionally considered to be 1 keV. This limit concerns the energy of the interacting particle. The lower energy limit of Penelope's applicability is generically indicated by its authors as "a few hundred electronvolts" [8]. The applicability of Geant4 low energy electromagnetic models based on the EADL, EEDL and EPDL data libraries was originally recommended for incident electron energies above 250 eV [175]; this recommendation was an "educated guess" rather than a rigorous estimate of validity of the theoretical cross section calculations tabulated in EEDL and EPDL. The first quantitative evaluation of the validity of electromagnetic cross sections based on EEDL below 1 keV is documented in [75]; this reference also documents the validation of two other electron ionization cross section models down to the scale of tens of electronvolts with respect to a wide collection of experimental data. These results suggest that the limit of validity of the independent atom assumption could be extended below 1 keV; nevertheless, further evidence, also concerning other processes, is needed before reaching a firm conclusion about the lower limit of validity of the independent atom assumption. Ultimately the judgment whether the accuracy achieved by the simulation is adequate depends on the requirements specific to each experimental application.

Molecular effects should be taken into account in particle transport, when the energy of the interacting particle falls below the limit of applicability of the independent atom assumption. Nevertheless, at the present time general purpose Monte Carlo models do not exist outside the independent atom scheme.

The compilations considered in the present paper are atomic data and, as discussed in Section IV-A, electron binding energies are known to be affected by the environment in which the atom finds itself. Current general purpose Monte Carlo codes for particle transport do not deal with effects determined by that environment, since, as discussed above, they treat all electromagnetic interactions based on the independent atom assumption. Experimentalists concerned with describing these effects in their simulations should not use general purpose Monte Carlo codes for particle transport.

It is worthwhile to stress that a more realistic description of material properties, not limited to atomic features, would not contribute by itself to improve the accuracy of the simulation, since it could not be incorporated in the current transport schemes of general purpose Monte Carlo codes. Accounting for molecular bindings would imply a major revision of the conceptual assumptions currently governing particle transport in general purpose Monte Carlo systems, and the development of a complete set of models of particle interactions in a new transport scheme.

Nevertheless, it is also worthwhile to stress that the independent atom assumption, so far adopted in Monte Carlo particle transport, successfully describes particle interactions with matter in a large number of simulation applications. All the simulation results based on general purpose Monte Carlo codes, which have been documented and validated in the literature to date, have been carried out in this scheme; many of them involve compounds.

The above discussion concerns electromagnetic interactions of particles with the medium; hadronic interactions are not considered, since nuclear processes are not related to the role of electron binding energies in particle transport.

X. CONCLUSION

A survey of compilations of atomic binding energies compilations used by general purpose Monte Carlo transport codes and other specialized software systems has been performed. Most compilations are based on experimental data; the only exception among those considered in this study is EADL, which is the result of theoretical calculations.

The accuracy of these compilation has been evaluated through direct comparisons with experimental data and through their effects on related physical quantities used in particle transport and experimental observables. An overview of the main findings from the various test cases is summarized in Table XV for convenience; it is not intended to replace the quantitative results and related discussions reported in the previous sections.

The results of this study show that no single compilation is ideal for all applications.

Direct comparisons with reference experimental data, which concern a subset of K, L, M and N shells, identify Williams' compilation, included in the X-ray Data Booklet and CRC Handbook of Physics and Chemistry, as the one best agreeing with experimental values. Regarding outer shells, ionization energies appear to be best reproduced by Carlson's compilation; Lotz's ionization energies are identical to Carlson's for elements with atomic number up to 92.

K and L shell X-ray energies are more accurately calculated based on the binding energies reported in the 1996 Table of Isotopes. With respect to these binding energies, the X-ray energies derived from the compilations by Bearden and Burr, Sevier and Williams do not exhibit any statistically significant disagreement in compatibility with average zero difference from experiment. Regarding the variance of such differences, the various compilations, with the exception of EADL, are equivalent to the 1996 Table of Isotopes in 60% to 79% of the transitions. X-ray energies based on EADL, although less accurate than those produced by other compilations, differ from the experimental references by less than 2% for most transitions: such an inaccuracy can be tolerable in some experimental applications, while others, where accuracy of simulated X-ray energies is important, should utilize the 1996 Table of Isotopes or other compilations providing better accuracy than EADL in this domain.

Total cross sections for electron impact ionization addressing the energy range below 1 keV (relevant to microdosimetry applications) are sensitive to the values of ionization potentials, while they are marginally influenced by inner shell binding energies. Lotz-Carlson's compilation and EADL modified to include NIST experimental ionization energies exhibit equivalent behaviour, while the use of EADL original ionization energies substantially decreases the accuracy of the cross section calculation.

K shell ionization cross sections by proton impact are sensitive to the binding energy values used in the ECPSSR calculation. All the empirical binding energy compilations produce results compatible with experimental measurements, while cross sections based on EADL show statistically significant worse accuracy. Binding energies also affect the calculation of ECPSSR cross sections for the L shell, but the differences are smaller than for the K shell; the uncertainties of L shell experimental data are too large to appreciate the effect of different binding energies in terms of modeling accuracy.

The simulation of Doppler broadening in Compton scattering appears insensitive to the choice of binding energies among the examined compilations.

Simulation applications with high precision requirements may profit from the results documented in this paper to identify the optimal set of binding energies for specific scenarios (e.g., material analysis, microdosimetry, PIXE etc.).

As no single compilation is suitable for all applications, it is highly desirable for simulation packages to allow experimentalists to choose which compilation to use for their application. This is much more easily possible in packages which read their binding energy data from file at runtime, rather than hard-coding it into the application binaries as in GEANT 3 and Geant4 *materials* package.

EADL binding energies appear consistently associated with worse accuracy in all the test cases analyzed in this paper. An evolution of EADL to better reflect the state-of-the-art would be desirable; it has already been advocated in [176] regarding the improvement of radiative transition probabilities. However, modifications to EADL should preserve the consistency with two other related data libraries, indices (Evaluated Electron Data Library) [36] and EPDL (Evaluated Photon Data Library) [37], as these compilations are intended to provide a consistent set of data for electron-photon transport calculations.

All the above summarized results should take into account the limitations discussed in Section IX.

ACKNOWLEDGMENT

The authors would like to thank CERN for support with the research described in this paper. The CERN Library, in particular T. Basaglia, provided helpful assistance and essential reference material for this study. The authors would also like to thank A. Buckley for proofreading the manuscript and valuable comments. The content of Section IX has been added per the request of the editors of the manuscript. The authors gratefully acknowledge the reuse of sentences suggested by Senior Editor Z. W. Bell of IEEE TRANSACTIONS ON NUCLEAR SCIENCE in Section IX and thank him for precious advice.

REFERENCES

[1] H. Hirayama, Y. Namito, A. F. Bielajew, S. J. Wilderman, and W. R. Nelson, The EGS5 code system Stanford, CA, 2006, SLAC-R-730 Rep.
[2] I. Kawrakow, E. Mainegra-Hing, D. W. O. Rogers, F. Tessier, and B. R. B. Walters, The EGSnrc Code System: Monte Carlo Simulation of Electron and Photon Transport NRCC Rep. PIRS-701, 2010.
[3] S. Agostinelli *et al.*, "Geant4—a simulation toolkit," *Nucl. Instrum. Methods Phys. Res. A*, vol. 506, no. 3, pp. 250–303, 2003.
[4] J. Allison *et al.*, "Geant4 developments and applications," *IEEE Trans. Nucl. Sci.*, vol. 53, no. 1, pp. 270–278, Feb. 2006.
[5] B. C. Franke, R. P. Kensek, and T. W. Laub, ITS5 Theory Manual, Sandia Natl. Lab Albuquerque, NM, 2004, Rep. SAND2004-4782.
[6] MCNP—A General Monte Carlo N-Particle Transport Code, Version 5 X-5 Monte Carlo Team, 2005, Los Alamos National Laboratory Rep. LA-UR-03-1987.
[7] J. S. Hendricks *et al.*, MCNPX, Version 26c, 2006, Los Alamos National Laboratory Rep. LA-UR-06-7991.
[8] J. Baro, J. Sempau, J. M. Fernández-Varea, and F. Salvat, "PENELOPE, an algorithm for Monte Carlo simulation of the penetration and energy loss of electrons and positrons in matter," *Nucl. Instrum. Methods Phys. Res. B*, vol. 100, no. 1, pp. 31–46, 1995.
[9] J. A. Bearden and A. F. Burr, "Reevaluation of X-ray atomic energy levels," *Rev. Mod. Phys.*, vol. 39, pp. 125–142, 1967.
[10] J. C. Slater, "One-electron energies of atoms, molecules, and solids," *Phys. Rev.*, vol. 98, pp. 1039–1945, 1955.
[11] B. Crasemann, K. R. Karim, and M. H. Chen, "Resource note: Theoretical atomic-electron binding energies," *Atom. Data Nucl. Data Tables*, vol. 36, no. 3, pp. 355–374, 1987.
[12] T. A. Carlson, *Photoelectron and Auger Spectroscopy*. New York: Plenum, 1975.
[13] S. T. Perkins *et al.*, "Tables and graphs of atomic subshell and relaxation data derived from the LLNL evaluated atomic data library (EADL) $Z = 1 - 100$," vol. 30, 1997, Lawrence Livermore National Laboratory, UCRL-50400.
[14] K. D. Sevier, "Atomic electron binding energies," *Atom. Data Nucl. Data Tables*, vol. 24, pp. 323–371, 1979.
[15] *Table of Isotopes*, R. B. Firestone and V. S. Shirley, Eds., 8th ed. New York: Wiley, 1996.
[16] *Table of Isotopes*, M. Lederer and V. S. e. Shirley, Eds., 7th ed. New York: Wiley, 1978.
[17] A. C. Thompson *et al., X-ray Data Booklet*, 3rd ed. Berkeley, CA: Lawrence Berkeley Nat. Lab, 2009.
[18] *CRC Handbook of Chemistry and Physics*, D. R. Lide, Ed., 90th ed. Boca Raton, FL: CRC Press, 2009.
[19] W. Lotz, "Electron binding energies in free atoms," *J. Opt. Soc. Amer.*, vol. 60, pp. 206–210, 1970.

[20] D. A. Shirley, R. L. Martin, S. P. Kowalczyk, F. R. McFeely, and L. Ley, "Core-electron binding energies of the first thirty elements," *Phys. Rev. B*, vol. 15, pp. 544–552, 1977.

[21] H. Siegbahn and L. Karlsson, "Photoelectron Spectroscopy, Corpuscles and Radiation in Matter I," in *Encyclopedia of Physics*, W. Mehlhorn, Ed. Berlin, Germany: Springer, 1982, vol. 31, pp. 215–467.

[22] F. P. Larkins, "Semiempirical Auger-electron energies for elements $10 \leq Z \leq 100$," *Atom. Data Nucl. Data Tables*, vol. 20, pp. 311–387, 1977.

[23] K. D. Sevier, *Appendix F, In: Low Energy Electron Spectrometry*. New York: Wiley-Interscience, 1972.

[24] F. T. Porter and M. S. Freedman, "Recommended atomic electron binding energies $1s0$ to $6p3/2$, for the heavy elements, $Z = 84$ to 103," *J. Phys. Chem. Ref. Data*, vol. 7, pp. 1267–1284, 1978.

[25] W. C. Martin, A. Musgrove, S. Kotochigova, and J. E. Sansonetti, Ground Levels and Ionization Energies for the Neutral Atoms [Online]. Available: http://www.nist.gov/physlab/data/ion_energy.cfm

[26] J. H. Scofield, "Radiative decay rates of vacancies in the K and L shells," *Phys. Rev. A*, vol. 18, pp. 9–16, 1969.

[27] J. H. Scofield, "Relativistic Hartree-Slater values for K and L X-ray emission rates," *Atom. Data Nucl. Data Tables*, vol. 14, pp. 121–137, 1974.

[28] J. H. Scofield, "K- and L-shell ionization of atoms by relativistic electrons," *Phys. Rev.*, vol. 179, pp. 963–970, 1978.

[29] J. H. Scofield, "Angular distribution of photoelectrons from polarized X-rays," *Phys. Scr.*, vol. 41, pp. 59–62, 1990.

[30] M. Cardona and L. E. Ley, *Photoemission in Solids I: General Principles*. Berlin, Germany: Springer-Verlag, 1978.

[31] J. C. Fuggle and N. Martensson, "Core-level binding energies in metals," *J. Electron Spectrosc. Relat. Phenom.*, vol. 21, pp. 275–281, 1980.

[32] W. R. Nelson, H. Hirayama, and D. W. O. Rogers, The EGS4 Code System, Stanford, CA, 1985, SLAC-265 Rep..

[33] , D. R. Lide, Ed., *CRC Handbook of Chemistry and Physics*, 73rd ed. Boca Raton, FL: , 1992.

[34] S. Chauvie, G. Depaola, V. Ivanchenko, F. Longo, P. Nieminen, and M. G. Pia, "Geant4 low energy electromagnetic physics," in *Proc. Computing in High Energy and Nuclear Physics*, Beijing, China, 2001, pp. 337–340.

[35] S. Chauvie *et al.*, "Geant4 low energy electromagnetic physics," in *Proc. IEEE Nuclear Science Symp. Conf. Rec.*, 2004, pp. 1881–1885.

[36] S. T. Perkins *et al.*, "Tables and graphs of electron-interaction cross sections from 10 eV to 100 GeV derived from the LLNL evaluated electron data library (EEDL)," vol. 31, 1997, Lawrence Livermore National Laboratory, UCRL-50400.

[37] D. Cullen *et al.*, "EPDL97, the evaluated photon data library," vol. 61, 1997, UCRL-50400.

[38] H. Abdelhwahed, S. Incerti, and A. Mantero, "New Geant4 cross section models for PIXE simulation," *Nucl. Instrum. Methods Phys. Res. B*, vol. 267, no. 1, pp. 37–44, 2009.

[39] A. Mantero *et al.*, "PIXE simulation in Geant4," *X-Ray Spectrom.*, vol. 40, no. PIXE 2010, pp. 135–140, 2011.

[40] M. G. Pia *et al.*, "PIXE simulation with Geant4," *IEEE Trans. Nucl. Sci.*, vol. 56, no. 6, pp. 3614–3649, Dec. 2009.

[41] Z. Liu and S. J. Cipolla, "Isics: A program for calculating K-, L- and M-shell cross sections from ECPSSR theory using a personal computer," *Comp. Phys. Comm.*, vol. 97, pp. 315–330, 1996.

[42] GEANT Detector Description and Simulation Tool, CERN Program Library Long Writeup W5013, 1995.

[43] V. M. Grishin, V. K. Ermilova, and S. K. Kotelnikov, "Ionization energy loss in very thin absorbers," *Nucl. Instrum. Methods*, vol. 309, no. 3, pp. 476–484, 1991.

[44] J. A. Maxwell, J. L. Campbell, and W. J. Teesdale, "The guelph PIXE software package," *Nucl. Instrum. Methods Phys. Res. B*, vol. 43, no. 2, pp. 218–230, 1989.

[45] J. L. Campbell, T. L. Hopman, J. A. Maxwell, and Z. Nejedly, "The guelph PIXE software package III: Alternative proton database," *Nucl. Instrum. Methods Phys. Res. B*, vol. 170, pp. 193–204, 2000.

[46] S. J. Cipolla, "ISICS2011, an updated version of ISICS: A program for calculation K-, L- and M-shell cross sections from PWBA and ECPSSR theories using a personal computer," *Comp. Phys. Comm.*, vol. 182, no. 11, pp. 2439–2440, 2011.

[47] G. Battistoni *et al.*, "The FLUKA code: Description and benchmarkin," in *Proc. American Institute of Physics Conf.*, 2007, vol. 896, pp. 31–49.

[48] A. Ferrari *et al.*, Fluka: a Multi-Particle Transport Code Geneva, Switzerland, 2005, Rep. CERN-2005-010, INFN/TC-05/11, SLAC-R-773.

[49] G. A. P. Cirrone *et al.*, "A goodness-of-fit statistical toolkit," *IEEE Trans. Nucl. Sci.*, vol. 51, no. 5, pp. 2056–2063, Oct. 2004.

[50] B. Mascialino, A. Pfeiffer, M. G. Pia, A. Ribon, and P. Viarengo, "New developments of the goodness-of-fit statistical toolkit," *IEEE Trans. Nucl. Sci.*, vol. 53, no. 6, pp. 3834–3841, Dec. 2006.

[51] S. Halas and T. Durakiewicz, "Work functions of elements expressed in terms of the Fermi energy and the density of free electrons," *J. Phys. Cond. Matter*, vol. 10, no. 48, pp. 10815–10826, 1998.

[52] T. J. Drummond, Work Functions of the Transition Metals and Metal Silicides, Albuquerque, NM, 1999, Sandia Rep. SAND99-0391J.

[53] C. J. Powell, "Formal databases for surface analysis: The current situation and future trends," *Surf. Interface Anal.*, vol. 17, pp. 308–314, 1991.

[54] C. J. Powell, "Elemental binding energies for X-ray photoelectron spectroscopy," *Appl. Surf. Sci.*, vol. 89, pp. 141–149, 1995.

[55] J. R. Rumble, Jr, D. M. Bickham, and C. J. Powell, "The NIST x-ray photoelectron spectroscopy database," *Surf. Interface Anal.*, vol. 19, pp. 241–246, 1992.

[56] A. N. Kolmogorov, "Sulla determinazione empirica di una legge di distribuzione," *Gior. Ist. Ital. Attuari*, vol. 4, pp. 83–91, 1933.

[57] N. V. Smirnov, "On the estimation of the discrepancy between empirical curves of distributions for two independent samples," 1939, Bull. Math. Univ. Moscou.

[58] T. W. Anderson and D. A. Darling, "Asymptotic theory of certain goodness of fit criteria based on stochastic processes," *Ann. Ma. St.*, vol. 23, pp. 193–212, 1952.

[59] T. W. Anderson and D. A. Darling, "A test of goodness of fit," *J. Amer. Stat. Assoc.*, vol. 49, pp. 765–769, 1954.

[60] H. Cramér, "On the composition of elementary errors. Second paper: statistical applications," *Skand. Aktuarietidskr.*, vol. 11, pp. 141–180, 1928.

[61] R. von Mises, *Wahrscheinlichkeitsrechnung und Ihre Anwendung in der Statistik und Theoretischen Physik*, F. Duticke, Ed. Leipzig, Germany: Leipzig, 1931, pp. 316–335.

[62] R. K. Bock and W. Krischer, *The Data Analysis BriefBook*. Berlin, Germany: Springer, 1998.

[63] C. D. Wagner, A. V. Naumkin, A. Kraut-Vass, J. W. Allison, C. J. Powell, and J. R. Rumble, Jr, NIST X-ray Photoelectron Spectroscopy Database [Online]. Available: http://srdata.nist.gov/xps/RecomEnergy.aspx?EnergyType=PE

[64] R. D. Deslattes *et al.*, "X-ray transition energies: new approach to a comprehensive evaluation," *Rev. Mod. Phys.*, vol. 75, pp. 35–99, 2003.

[65] S. Guatelli *et al.*, "Validation of Geant4 Atomic Relaxation against the NIST Physical Reference Data," *IEEE Trans. Nucl. Sci.*, vol. 54, no. 3, pp. 594–603, Jun. 2007.

[66] S. Guatelli, A. Mantero, B. Mascialino, P. Nieminen, and M. G. Pia, "Geant4 atomic relaxation," *IEEE Trans. Nucl. Sci.*, vol. 54, no. 3, pp. 585–593, Jun. 2007.

[67] R. A. Fisher, "On the interpretation of χ^2 from contingency tables, and the calculation of P," *J. Royal Stat. Soc.*, vol. 85, no. 1, pp. 87–94, 1922.

[68] K. Pearson, "On the χ^2 test of goodness of fit," *Biometrika*, vol. 14, no. 1–2, pp. 186–191, 1922.

[69] F. Yates, "Contingency table involving small numbers and the χ^2 test," *J. Royal Stat. Soc. Suppl.*, vol. 1, pp. 217–235, 1934.

[70] Y. K. Kim and M. E. Rudd, "Binary-encounter-dipole model for electron-impact ionization by electron impact," *Phys. Rev. A*, vol. 50, pp. 3954–3967, 1994.

[71] W. Brandt and G. Lapicki, "Energy-loss effect in inner-shell Coulomb ionization by heavy charged particles," *Phys. Rev. A*, vol. 23, pp. 1717–1729, 1981.

[72] H. Deutsch and T. D. Märk, "Calculation of absolute electron impact ionization cross-section functions for single ionization of He, Ne, Ar, Kr, Xe, N and F," in *Int. J. Mass Spectrom. Ion Proc.*, 1987, vol. 79, pp. R1–R8.

[73] H. Seo, M. G. Pia, P. Saracco, and C. H. Kim, "Design, development and validation of electron ionization models for nano-scale simulation," in *Proc. SNA-Monte Carlo Conf.*, Tokyo, Japan, 2010.

[74] H. Seo, M. G. Pia, P. Saracco, and C. H. Kim, "Ionization models for nano-scale simulation," in *Proc. IEEE Nuclear Science Symp.*, Knoxville, TN, 2010.

[75] H. Seo, M. G. Pia, P. Saracco, and C. H. Kim, "Ionization cross sections for low energy electron transport," *IEEE Trans. Nucl. Sci.*, vol. 58, no. 6, pp. 3219–3245, Dec. 2011.

[76] H. Deutsch, P. Scheier, S. Matt-Leubner, K. Becker, and T. D. Märk, "A detailed comparison of calculated and measured electron-impact ionization cross sections of atoms using the Deutsch-Märk (DM) formalism," *Int. J. Mass Spectrom.*, vol. 243, pp. 215–221, 2005.

[77] H. Deutsch, P. Scheier, S. Matt-Leubner, K. Becker, and T. D. Märk, "Erratum to a detailed comparison of calculated and measured electron-impact ionization cross sections of atoms using the Deutsch-Märk (DM) formalism," *Int. J. Mass Spectrom.*, vol. 246, p. 113, 2005.

[78] D. Margreiter, H. Deutsch, and T. D. Märk, "A semiclassical approach to the calculation of electron impact ionization cross-sections of atoms: From hydrogen to uranium," *Int. J. Mass Spectrom. Ion Processes*, vol. 139, pp. 127–139, 1994.

[79] L. J. Kieffer and G. H. Dunn, "Electron impact ionization cross-section data for atoms, atomic ions, and diatomic molecules: I. experimental data," *Rev. Mod. Phys.*, vol. 38, no. 1, pp. 1–35, 1966.

[80] M. A. Ali, Y. K. Kim, W. Hwang, N. M. Weinberger, and M. E. Rudd, "Electron-impact total ionization cross sections of silicon and germanium hydrides," *J. Chem. Phys.*, vol. 106, no. 23, pp. 9602–9608, 1997.

[81] Y. K. Kim, J. Migdalek, W. Siegel, and J. Bieron, "Electron-impact ionization cross section of rubidium," *Phys. Rev. A*, vol. 57, pp. 246–254, 1998.

[82] Y. K. Kim, W. R. Johnson, and M. E. Rudd, "Cross sections for singly differential and total ionization of helium by electron impact," *Phys. Rev. A*, vol. 61, p. 034702, 2000.

[83] Y. K. Kim, J. P. Santos, and F. Parente, "Extension of the binary-encounter-dipole model to relativistic incident electrons," *Phys. Rev. A*, vol. 62, p. 052710, 2000.

[84] Y. K. Kim and P. M. Stone, "Ionization of boron, aluminum, gallium, and indium by electron impact," *Phys. Rev. A*, vol. 64, p. 052707, 2001.

[85] Y. K. Kim and J. P. Desclaux, "Ionization of carbon, nitrogen, and oxygen by electron impact," *Phys. Rev. A*, vol. 66, p. 012708, 2002.

[86] Y. K. Kim and P. M. Stone, "Ionization of silicon, germanium, tin and lead by electron impact," *J. Phys. B, At. Mol. Opt. Phys.*, vol. 40, pp. 1597–1661, 2007.

[87] M. A. Ali and Y. K. Kim, "Ionization cross sections by electron impact on halogen atoms, diatomic halogen and hydrogen halide molecules," *J. Phys. B, At. Mol. Opt. Phys.*, vol. 41, p. 145202, 2008.

[88] M. B. Shah, D. S. Elliott, and H. B. Gilbody, "Pulsed crossed-beam st0udy of the ionization of atomic hydrogen by electron impact," *J. Phys. B, At. Mol. Phys.*, vol. 20, pp. 3501–3514, 1987.

[89] W. L. Fite and R. T. Brackmann, "Collisions of electrons with hydrogen atoms. I. ionization," *Phys. Rev.*, vol. 112, no. 4, pp. 1141–1151, 1958.

[90] E. W. Rothe, L. L. Marino, R. H. Neynaber, and S. M. Trujillo, "Electron impact ionization of atomic hydrogen and atomic oxygen," *Phys. Rev.*, vol. 125, no. 2, pp. 582–583, 1962.

[91] R. Rejoub, B. G. Lindsay, and R. F. Stebbings, "Determination of the absolute partial and total cross sections for electron-impact ionization of the rare gases," *Phys. Rev. A*, vol. 65, p. 042713, 2002.

[92] M. B. Shah, D. S. Elliott, P. McCallion, and H. B. Gilbody, "Single and double ionization of helium by electron impact," *J. Phys. B, At. Mol. Opt. Phys.*, vol. 21, pp. 2751–2761, 1988.

[93] D. Rapp and P. Englander-Golden, "Total cross sections for ionization and attachment in gases by electron impact," *Phys. Rev. A*, vol. 43, no. 5, pp. 1464–1479, 1965.

[94] B. L. Schram, A. J. H. Boerboom, and J. Kistemaker, "Partial ionization cross sections of noble gases for electrons with energy 0.5–16 keV," *Physica*, vol. 32, pp. 185–196, 1966.

[95] K. Stephan, H. Helm, and T. D. Märk, "Mass spectrometric determination of partial electron impact ionization cross sections of He, Ne, Ar and Kr from threshold up to 180 eV," *J. Chem. Phys.*, vol. 73, no. 8, pp. 3763–3778, 1980.

[96] E. Krishnakumar and S. K. Srivastava, "Ionization cross sections of rare-gas atoms by electron impact," *J. Phys. B, At. Mol. Opt. Phys.*, vol. 21, pp. 1055–1082, 1988.

[97] R. G. Montague, M. F. A. Harrison, and A. C. H. Smith, "A measurement of the cross section for ionization of helium by electron impact using a fast crossed beam technique," *J. Phys. B, At. Mol. Phys.*, vol. 17, pp. 3295–3310, 1984.

[98] P. Nagy, A. Skutlartz, and V. Schmidt, "Absolute onization cross sections for electron impact in rare gases," *J. Phys. B, At. Mol. Phys.*, vol. 13, pp. 1249–1267, 1980.

[99] R. C. Wetzel, F. A. Baiocchi, T. R. Hayes, and R. S. Freund, "Absolute cross sections for electron-impact ionization of the rare-gas atoms by the fast neutral beam method," *Phys. Rev. A*, vol. 35, no. 2, pp. 559–577, 1987.

[100] R. H. McFarland and J. D. Kinney, "Absolute cross sections of Li and other alkali metal atoms for ionization by electrons," *Phys. Rev.*, vol. 137, no. 4A, pp. 1058–1061, 1965.

[101] I. P. Zapesochnyi and I. S. Aleksakhin, "Ionization of alkali metal atoms by slow electrons," *Sov. Phys. JETP*, vol. 28, no. 1, pp. 41–45, 1969.

[102] R. Jalin, R. Hagemann, and R. Botter, "Absolute electron impact ionization cross sections of li in the energy range from 100 to 2000 eV," *J. Chem. Phys.*, vol. 59, no. 2, pp. 952–959, 1973.

[103] E. Brook, M. F. A. Harrison, and A. C. H. Smith, "Measurements of the electron impact ionization cross sections of He, C, O and N atoms," *J. Phys. B, Atom. Molec. Phys.*, vol. 11, no. 17, pp. 3115–3132, 1978.

[104] A. C. H. Smith, E. Caplinger, R. H. Neynaber, E. W. Rothe, and S. M. Trujillo, "Electron impact ionization of atomic nitrogen," *Phys. Rev.*, vol. 127, no. 5, pp. 1647–1649, 1962.

[105] J. R. Peterson, *Atomic Collision Processes*, M. R. C. McDowell, Ed. Amsterdam, The Netherlands: North Holland, 1964, pp. 465–473.

[106] W. R. Thompson, M. B. Shah, and H. B. Gilbody, "Single and double ionization of atomic oxygen by electron impact," *J. Phys. B, At. Mol. Opt. Phys.*, vol. 28, pp. 1321–1330, 1995.

[107] E. C. Zipf, "The ionization of atomic oxygen by electron impact," *Planet. Space Sci.*, vol. 33, no. 11, pp. 1303–1307, 1985.

[108] W. L. Fite and R. T. Brackmann, "Ionization of atomic oxygen on electron impact," *Phys. Rev.*, vol. 113, pp. 815–816, 1959.

[109] T. R. Hayes, R. C. Wetzel, and R. S. Freund, "Absolute electron-impact-ionization cross-section measurements of the halogen atoms," *Phys. Rev. A*, vol. 35, no. 2, pp. 578–584, 1987.

[110] B. Adamczyk, A. J. H. Boerboom, B. L. Schram, and J. Kistemaker, "Partial ionization cross sections of he, ne, H_2, and CH_4 for electrons from 20 to 500 eV," *J. Chem. Phys.*, vol. 44, pp. 4640–4642, 1966.

[111] D. P. Almeida, A. C. Fontes, and C. F. L. Godinho, "Electron-impact ionization cross section of neon $(\sigma_{n+}, n = 1 - 5)$," *J. Phys. B, At. Mol. Opt. Phys.*, vol. 28, pp. 3335–3345, 1995.

[112] J. Fletcher and I. R. Cowling, "Electron impact ionization of neon and argon," *J.Phys. B, At. Mol. Phys.*, vol. 6, pp. L258–L261, 1973.

[113] A. A. Sorokin, L. A. Shmaenok, and S. V. Bobashev, "Measurements of electron-impact ionization cross sections of neon by comparison with photoionization," *Phys. Rev. A*, vol. 58, no. 4, pp. 2900–2910, 1998.

[114] G. O. Brink, "Absolute ionization cross sections of the alkali metals," *Phys. Rev.*, vol. 134, no. 2A, pp. A345–A346, 1964.

[115] K. Fujii and S. K. Srivastava, "A measurement of the electron-impact ionization cross section of sodium," *J. Phys. B*, vol. 28, pp. L559–L563, 1995.

[116] A. R. Johnston and P. D. Burrow, "Electron-impact ionization of Na," *Phys. Rev. A*, vol. 51, no. 3, pp. R1735–R1737, 1995.

[117] W. S. Tan, Z. Shi, C. H. Ying, and L. Vuskovic, "Electron-impact ionization of laser-excited sodium atom," *Phys. Rev. A*, vol. 54, no. 5, pp. R3710–R3713, 1996.

[118] R. S. Freund, R. C. Wetzel, R. J. Shul, and T. R. Hayes, "Cross-section measurements for electron-impact ionization of atoms," *Phys. Rev. A*, vol. 41, no. 7, pp. 3575–3595, 1990.

[119] R. F. Boivin and S. K. Srivastava, "Electron-impact ionization of Mg," *J. Phys. B, At. Mol. Opt. Phys.*, vol. 31, pp. 2381–2394, 1998.

[120] F. Karstensen and M. Schneider, "Absolute cross sections for single and double ionization of Mg atoms by electron impact," *J. Phys. B, At. Mol. Phys.*, vol. 11, no. 1, pp. 167–172, 1978.

[121] P. McCallion, M. B. Shah, and H. B. Gilbody, "Multiple ionization of magnesium by electron impact," *J. Phys. B, At. Mol. Opt. Phys.*, vol. 25, no. 5, pp. 1051–1060, 1992.

[122] L. A. Vainshtein, V. I. Ochkur, V. I. Rakhovskii, and A. M. Stepanov, "Absolute values of electron impact ionization cross sections for magnesium, calcium, strontium and barium," *Sov. Phys. JETP*, vol. 34, no. 2, pp. 271–275, 1972.

[123] Y. Okuno, K. Okuno, Y. Kaneko, and I. Kanomata, "Absolute measurement of total ionization cross section of Mg by electron impact," *J. Phys. Soc. Jpn.*, vol. 29, pp. 164–172, 1970.

[124] D. G. Golovach, A. N. Drozdov, V. I. Rakhovskii, and V. M. Shustryakov, "Measurment of the ionization cross section of aluminum atoms by electronic impact," *Meas. Tech. (USSR)*, vol. 30, pp. 587–589, 1987.

[125] L. L. Shimon, E. I. Nepiipov, and I. P. Zapesochnyi, "Effective total electron-impact ionization cross sections for aluminum, gallium, indium and thallium," *Sov. Phys. Tech. Phys.*, vol. 20, no. 3, p. 434, 1975.

[126] D. L. Ziegler, J. H. Newman, L. N. Goeller, K. A. Smith, and R. F. Stebbings, "Single and multiple ionization of sulfur atoms by electron impact," *Planet. Space Sci.*, vol. 30, no. 12, pp. 1269–1274, 1982.

[127] H. C. Straub, P. Renault, B. G. Lindsay, K. A. Smith, and R. F. Stebbings, "Absolute partial and total cross sections for electron-impact ionization of argon from threshold to 1000 eV," *Phys. Rev. A*, vol. 52, no. 2, pp. 1115–1124, 1995.

[128] B. L. Schram, "Partial ionization cross sections of noble gases for electrons with energy 0.5–18 keV," *Physica*, vol. 32, pp. 197–208, 1966.
[129] P. McCallion, M. B. Shah, and H. B. Gilbody, "A crossed beam study of the multiple ionization of argon by electron impact," *J. Phys. B, At. Mol. Opt. Phys.*, vol. 25, no. 5, pp. 1061–1071, 1992.
[130] C. Ma, C. R. Sporleder, and R. A. Bonham, "A pulsed electron beam time of flight apparatus for measuring absolute electron impact ionization and dissociative ionization cross sections," *Rev. Sci. Instrum.*, vol. 62, pp. 909–923, 1991.
[131] Y. P. Korchevoi and A. M. Przonski, "Effective electron impact excitation and ionization cross sections for cesium, rubidium, and potassium atoms in the pre-threshold region," *Sov. Phys. JETP*, vol. 24, no. 6, pp. 1089–1092, 1967.
[132] K. J. Nygaard, "Electron impact autoionization in heavy alkali metals," *Phys. Rev. A*, vol. 11, no. 4, pp. 1475–1478, 1975.
[133] R. H. McFarland, "Electron-impact ionization measurements of surface-ionizable atoms," *Phys. Rev.*, vol. 159, no. 1, pp. 20–26, 1967.
[134] Y. Okuno, "Ionization cross sections of ca, sr and ba by electron impact," *J. Phys. Soc. Jpn.*, vol. 31, no. 4, pp. 1189–1195, 1971.
[135] M. Schneider, "Measurement of absolute ionization cross sections for electron impact," *J. Phys. D, Appl. Phys.*, vol. 7, pp. L83–L86, 1974.
[136] V. J. Rakhovski and A. M. Stepanov, "Absolute values of the apparent cross section for calcium ionization by electron collision," *High Temp.*, vol. 7, pp. 1001–1003, 1969.
[137] M. B. Shah, P. McCallion, K. Okuno, and H. B. Gilbody, "Multiple ionization of iron by electron impact," *J. Phys. B, At. Mol. Opt. Phys.*, vol. 26, pp. 2393–1401, 1993.
[138] M. A. Bolorizadeh, C. J. Patton, M. B. Shah, and H. B. Gilbody, "Multiple ionization of copper by electron impact," *J. Phys. B, At. Mol. Opt. Phys.*, vol. 27, pp. 175–183, 1994.
[139] S. I. Pavlov, V. I. Rakhovskii, and G. M. Fedorova, "Measurement of cross sections for ionization by electron impact at low vapor pressures," *Sov. Phys. JETP*, vol. 25, p. 12, 1967.
[140] J. M. Schroeer, D. H. Gunduz, and S. Livingston, "Electron impact ionization cross sections of cu and au between 40 and 250 eV, and the velocity of evaporated atoms," *J. Chem. Phys.*, vol. 58, no. 11, pp. 5135–5140, 1973.
[141] R. F. Pottie, "Cross sections for ionization by electrons. I. absolute ionization cross sections of zn, cd, and Te_2. II. Comparison of theoretical with experimental values for atoms and molecules," *J. Chem. Phys.*, vol. 44, no. 3, pp. 916–922, 1966.
[142] R. J. Shul, R. C. Wetzel, and R. S. Freund, "Electron-impact-ionization cross section of the ga and in atoms," *Phys. Rev. A*, vol. 39, no. 11, pp. 5588–5596, 1989.
[143] L. A. Vainshtein, D. G. Golovach, V. I. Ochkur, V. I. Rakhovskii, N. M. Rumyantsev, and V. M. Shustryakov, "Cross sections for ionization of gallium and indium by electrons," *Sov. Phys. JETP*, vol. 66, no. 1, pp. 36–39, 1987.
[144] C. J. Patton, K. O. Lozhkin, M. B. Shah, J. Geddes, and H. B. Gilbody, "Multiple ionization of gallium by electron impact," *J. Phys. B, At. Mol. Opt. Phys.*, vol. 29, pp. 1409–1417, 1996.
[145] K. J. Nygaard and Y. B. Hahn, "Total electron impact ionization cross section in rubidium from threshold to 250 eV," *J. Chem. Phys.*, vol. 58, no. 8, pp. 3493–3499, 1973.
[146] R. S. Schappe, T. Walker, L. W. Anderson, and C. C. Lin, "Absolute electron-impact ionization cross section measurements using a magneto-optical trap," *Phys. Rev. Lett.*, vol. 76, no. 23, pp. 4328–4331, 1996.
[147] C. K. Crawford and K. I. Wang, "Electron-impact ionization cross sections for silver," *J. Chem. Phys.*, vol. 47, pp. 4667–4669, 1967.
[148] K. Franzreb, A. Wucher, and H. Oechsner, "Absolute cross sections for electron impact ionization of Ag_2," *Z. Phys. D*, vol. 19, pp. 77–79, 1991.
[149] S. S. Lin and F. E. Stafford, "Electron-impact ionization cross sections. IV. group IVb atoms," *J. Chem. Phys.*, vol. 47, pp. 4664–4666, 1967.
[150] A. P. Lyubimov, S. I. Pavlov, V. I. Rakhovskii, and N. G. Zaitseva, "Procedure for measuring the ionization cross sections and ionization coefficients of metal atoms," *Bull. Acad. USSR. Phys. Ser.*, vol. 17, p. 1033, 1963.
[151] D. Mathur and C. Badrinathan, "Ionization of xenon by electrons: Partial cross sections for single, double and triple ionization," *Phys. Rev. A*, vol. 35, no. 3, pp. 1033–1042, 1987.
[152] K. Stephan and T. D. Märk, "Absolute partial electron impact ionization cross sections of Xe from threshold up to 180 eV," *J. Chem. Phys.*, vol. 81, no. 7, pp. 3116–3117, 1984.
[153] H. Heil and B. Scott, "Cesium ionization cross section from threshold to 50 eV," *Phys. Rev.*, vol. 145, no. 1, pp. 279–284, 1966.
[154] K. J. Nygaard, "Electron-impact ionization cross section in cesium," *J. Chem. Phys.*, vol. 49, no. 5, pp. 1995–2002, 1968.
[155] J. M. Dettmann and F. Karstensen, "Absolute ionization functions for electron impact with barium," *J. Phys. B, At. Mol. Phys.*, vol. 15, pp. 287–300, 1982.
[156] S. Yagi and T. Nagata, "Absolute total and partial cross-sections for ionization of ba and eu atoms by electron impact," *J. Phys. Soc. Jpn.*, vol. 69, no. 5, pp. 1374–1383, 2000.
[157] D. G. Golovach, V. I. Rakhovskii, and V. M. Shustryakov, "Apparatus for measurement of electronic-ionization cross sections of metal atoms," *Instrum. Exp. Tech.*, vol. 29, pp. 1396–1399, 1987.
[158] S. Yagi and T. Nagata, "Absolute total and partial cross sections for ionization of free lanthanide atoms by electron impact," *J. Phys. Soc. Jpn.*, vol. 70, no. 9, pp. 2559–2567, 2001.
[159] L. L. Shimon, P. N. Volovich, and M. M. Chiriban, "Multiple ionization of samarium, europium, thulium, and ytterbium atoms by electrons," *Sov. Phys. Tech. Phys.*, vol. 34, no. 11, pp. 1264–1266, 1989.
[160] W. Bleakney, "Probability and critical potentials for the formation of multiply charged ions in Hg vapor by electron impact," *Phys. Rev.*, vol. 35, no. 2, pp. 139–148, 1930.
[161] P. C. E. McCartney, M. B. Shah, J. Geddes, and H. B. Gilbody, "Multiple ionization of lead by electron impact," *J. Phys. B, At. Mol. Opt. Phys.*, vol. 31, pp. 4821–4831, 1998.
[162] S. I. Pavlov and G. I. Stotskii, "Single and multiple ionization of lead atoms by electrons," *Sov. Phys. JETP*, vol. 31, no. 1, pp. 61–64, 1970.
[163] G. M. Beilina, S. I. Pavlov, V. I. Rakhovskii, and O. D. Sorokaletov, "Measurement of electron impact ionization functions for metal atoms," *J. Appl. Mechan. Tech. Phys.*, vol. 2, pp. 86–88, 1965.
[164] J. B. Wareing and K. T. Dolder, "A measurement of the cross section for ionization of Li^{+} to Li^{2+} by electron impact," in *Proc. Phys. Soc.*, 1967, vol. 91, pp. 887–893.
[165] J. C. Halle, H. H. Lo, and W. L. Fite, "Ionization of uranium atoms by electron impact," *Phys. Rev. A*, vol. 23, no. 4, pp. 1708–1716, 1981.
[166] E. Merzbacher and H. Lewis, *Handbuch der Physik*. Berlin, Germany: Springer, 1958, vol. 34, pp. 166–192.
[167] M. Batic, S. J. Cipolla, and M. G. Pia, Isicsoo: A Class for the Calculation of Ionisation Cross Sections From PWBA and ECPSSR Theory Comp. Phys. Comm [Online]. Available: http://arxiv.org/abs/1110.0613
[168] H. Paul and J. Sacher, "Fitted empirical reference cross sections for K-shell ionization by protons," *Atom. Data Nucl. Data Tab.*, vol. 42, pp. 105–156, 1989.
[169] R. S. Sokhi and D. Crumpton, "Experimental L-shell X-ray production and ionization cross sections for proton impact," *Atom. Data Nucl. Data Tables*, vol. 30, pp. 49–124, 1984.
[170] I. Orlic, J. Sow, and S. M. Tang, "Experimental L-shell X-ray production and ionization cross sections for proton impact," *Atom. Data Nucl. Data Tables*, vol. 56, pp. 159–210, 1994.
[171] Y. Namito, S. Ban, and H. Hirayama, "Implementation of the Doppler broadening of a Compton-scattered photon into the EGS4 code," *Nucl. Instrum. Methods Phys. Res. A*, vol. 349, pp. 489–494, 1994.
[172] A. Sood, Doppler Energy Broadening for Incoherent Scattering in MCNP5, Part I Los Alamos, NM, 2004, Rep. LA-UR- 04-0487.
[173] F. Longo, L. Pandola, and M. G. Pia, "New Geant4 developments for Doppler broadening simulation in Compton scattering—development of charge transfer simulation models in Geant4," in *Proc. IEEE Nuclear Science Symp. Conf. Rec.*, 2008, pp. 2865–2868.
[174] A. Zoglauer *et al.*, "Doppler broadening as a lower limit to the angular resolution of next generation Compton telescopes," in *Proc. SPIE*, 2003, vol. 4581, pp. 1302–1309.
[175] J. Apostolakis, S. Giani, M. Maire, P. Nieminen, M. G. Pia, and L. Urban, "Geant4 low energy electromagnetic models for electrons and photons," INFN/AE-99/18, Frascati, Italy, 1999.
[176] M. G. Pia, P. Saracco, and M. Sudhakar, "Validation of K and L shell radiative transition probability calculations," *IEEE Trans. Nucl. Sci.*, vol. 56, no. 6, pp. 3650–3661, Dec. 2009.